



Original article

Intranasal hydrogel of armodafinil hydroxypropyl- β -cyclodextrin inclusion complex for the treatment of post-traumatic stress disorder



Ge Ou^{a,b,c}, Qian Li^{c,d}, Lin Zhu^c, Yuanyuan Zhang^{c,d}, Yijing Liu^{c,d}, Xin Li^{b,*}, Lina Du^{c,d,*}, Yiguang Jin^c

^a Medical School of Chinese PLA, Beijing 100853, China

^b Pharmacy Department, Chinese PLA General Hospital, Beijing 100853, China

^c Department of Pharmaceutical Sciences, Beijing Institute of Radiation Medicine, Beijing 100850, China

^d School of Medicine, Shandong University of Traditional Chinese Medicine, Jinan 250355, China

ARTICLE INFO

Article history:

Received 16 July 2021

Accepted 12 January 2022

Available online 19 January 2022

Keywords:

Post-traumatic stress disorder (PTSD)

Armodafinil

Administration

Intranasal

Hydrogels

Pharmacokinetics

Tissue distribution

ABSTRACT

Armodafinil inclusion complex (AIC) hydrogel was prepared and evaluated for its therapeutic effect on Post-traumatic Stress Disorder (PTSD). After computer simulation and physicochemical property investigation, the AIC was formed by lyophilization of armodafinil with ethanol as solvent and hydroxypropyl-beta-cyclodextrin (HP- β -CD) aqueous solution, in which the molar ratio of armodafinil and HP- β -CD was 1–1. The AIC encapsulation efficiency (EE) was $(90.98 \pm 3.72)\%$ and loading efficiency (LE) was $(13.95 \pm 0.47)\%$ and it increased the solubility of armodafinil in aqueous solution to 21 times. AIC hydrogel was prepared by adding AIC to methylcellulose (MC) hydrogels (3.33% w/v), and its higher drug release amount and slower release rate were testified by the *in-vitro* release assay and the rheological test. The mucosa irritation of AIC hydrogel was also evaluated. Healthy group, Model group, Sertraline group with 30 mg/kg sertraline gavage, AIC Hydrogel group with 20 mg/kg AIC hydrogel intranasal administration and AIC Aqueous Solution group with 20 mg/kg AIC aqueous solution gavage were set up for the treatment of mice with PTSD generated from foot shock method. Based on freezing response test in fear-conditioning box and open field test, compared with other groups, PTSD mice in AIC Hydrogel group showed significant improvement in behavioral parameters after 11 days of continuous drug administration and 5 days of drug withdrawal. After sacrifice, the plasma CORT level of PTSD mice in AIC Hydrogel group was elevated compared to Model group. Besides, the western blot (WB) of hippocampal brain-derived neurotrophic factor (BDNF) and amygdala dopamine transporter (DAT) immunohistochemistry sections indicated that AIC hydrogel had a protective effect on the brain tissue of PTSD mice. The brain targeting of intranasal administration was evaluated by fluorescence imaging characteristics of Cy7 hydrogel in the nasal route of drug administration, pharmacokinetics and *in-vivo* distribution of armodafinil. In short, AIC hydrogel is a promising formulation for the treatment of PTSD based on its high brain delivery and anti-PTSD effect.

© 2022 The Authors. Published by Elsevier B.V. on behalf of King Saud University. This is an open access article under the CC BY-NC-ND license (<http://creativecommons.org/licenses/by-nc-nd/4.0/>).

* Corresponding authors at: Pharmacy Department, Chinese PLA General Hospital, 28 Fuxing Road, Haidian District, Beijing 100853, China (X. Li). Department of Pharmaceutical Sciences, Beijing Institute of Radiation Medicine, 27 Taiping Road, Haidian District, Beijing 100850, China (L. Du).

E-mail addresses: doublelixin@outlook.com (X. Li), dulina@188.com (L. Du).

Peer review under responsibility of King Saud University.



1. Introduction

Post-traumatic stress disorder (PTSD) is a debilitating anxiety disorder. It is defined by the Diagnostic and Statistical Manual of Mental Disorders (DSM-V) as manifested primarily by four syndromes: intrusion, avoidance of reminders, altered cognitions and mood, altered arousal and reactivity (Ferland et al., 2016). This chronic disease afflicts a large number of individuals who do not improve significantly on available therapies and increases the risk of suicide, psychological disorders, cardiovascular disease, and cognitive impairment (Feduccia et al., 2019). Currently, only selective serotonin reuptake inhibitors (SSRIs), i.e., sertraline and paroxetine, are used for the treatment of PTSD in Europe and the United

States (Sartori and Singewald, 2019). However, the Side effects of SSRIs including neuroticism at the beginning of treatment, blunted emotions, gastrointestinal discomfort, insomnia, and sexual dysfunction, were remarkable, along with the disadvantages of slow onset and uncertain efficacy (Stübner et al., 2018). It is urgent to develop novel drugs and formulations for the treatment of PTSD.

Modafinil and armodafinil (an R-isomer of modafinil with longer plasma half-life than modafinil) are commonly used to treat obstructive apnea syndrome, narcolepsy, or shift work sleep disorder as wakefulness-promoting drugs (Chapman et al., 2016) (Fig. 1). Since 2012, these two drugs have formally entered phase 2/3 clinical trials (NCT01726088, ClinicalTrials.gov) as potential new drugs for the treatment of PTSD. The two drugs are slightly soluble in water and are used orally via capsules only. Compared to modafinil, armodafinil is characterized by smaller fluctuations in drug concentrations in-vivo and longer maintenance of drug concentrations, and therefore has better drug therapeutic potential (Darwish et al., 2009). Armodafinil was proved to be a promising therapeutic drug for PTSD treatment.

The Blood Brain Barrier (BBB) is the term used to describe the unique properties of the microvascular system in the Central Nervous System (CNS). This strict restriction is essential to ensure proper neuronal function by protecting the CNS from toxins, pathogens, inflammation, injury, and disease. However, during the treatment of CNS diseases, this limitation reversely becomes a barrier to drug delivery to reach the CNS. Drugs are restricted to cross the BBB unless under the condition of <400 Da molecular weight and non-polar non-polycyclic structure (Ghose et al., 2012). Thus, the therapeutic effect of armodafinil in PTSD, a CNS disorder, could be limited via oral or intravenous administration.

Intranasal administration is a method of drug delivery that bypasses the BBB and targets it into the brain by administering the drug in the nasal cavity. The nasal cavity has been divided into a respiratory zone near the nostrils and an olfactory zone locating deep inside the nostrils (Sahin-Yilmaz and Naclerio, 2011). In the respiratory zone, the drug is absorbed through the epithelium of the nasal airway and then enters the brain via the trigeminal nerve (Lochhead and Thorne, 2012). In the olfactory zone, the drug can enter the brain via the supporting cells or olfactory sensory neurons (Thorne et al., 2008). Thus, the distribution of the drug within the central nervous system is increased and the therapeutic effect is improved even with a relatively small dosage administration. In clinical studies of patients with schizophrenia, olanzapine was administered in nasal cavity loaded in polyglycolic acid hydrogel. The preparation increased the content of olanzapine in brain by

10 times compared with olanzapine aqueous solution. In clinical studies of Alzheimer's disease (AD), insulin was targeted to the brain by intranasal administration of insulin gel, improving cognition of AD patients, and preventing blood insulin level from increasing (Hamidovic et al., 2017).

Cyclodextrins are a group of cyclic oligosaccharides consisting of 6–8 α -D-glucoside units linked at the α -(1,4) bond position, which have better mucosal penetration properties and improve drug delivery in vivo (Davis and Brewster, 2004). Hydroxypropyl- β -Cyclodextrin (HP- β -CD) is a new generation of β -cyclodextrin derivatives (Fig. 1). The unique hydroxypropyl breaks the circular hydrogen bond in β -cyclodextrin molecules, so that enhances the water solubility of cyclodextrin molecules while maintaining the β -cyclodextrin cavity. In order to improve the aqueous solubility and mucosal penetration of armodafinil, AIC could be prepared by forming hydrogen bonds between the sulfinyl bond in armodafinil and the hydroxyl bond of HP- β -CD through lyophilization. Methylcellulose (MC), a water-soluble polysaccharide cellulose derivative, could form a hydrogel for cross-linking injection under the condition of about 37 °C, providing a cross-linked bio adhesive scaffold for long retention on nasal mucosa (Niemczyk-Soczynska et al., 2019). As a physically cross-linked hydrogel, MC does not generate and release heat, so that the cells or tissues around the target organ and the predicted therapeutic efficacy of the drug will not be affected (Dimatteo et al., 2018). After adding AIC to MC, AIC can be uniformly distributed in the voids of the hydrogel formed by MC to make AIC hydrogel, thus achieving the goal of longer retention time of armodafinil in the nasal cavity and more drug targeting into the brain.

The main PTSD models established for rodents include time-dependent sensitization, forced swimming, confinement stimulation, single prolonged stress, predator-based psychosocial stress, social isolation, and foot shock method (Zoladz et al., 2012). Foot shock method is a widely used stressor in animal models of PTSD, which reappears some core symptoms of PTSD, including avoidance, anxious behavior (Louvar et al., 2005), irritability, aggression, repetitive experience (Pynoos et al., 1996) and changes in sleep structure (Pawlyk et al., 2005). The widely used combination of foot shock method and repetitive experience in the process of stimulation is more in line with the disease process of human PTSD symptoms (Tanaka et al., 2019).

In this research, AIC hydrogel as a novel preparation was designed, and experiments concerning behavior, PTSD-related hormonal and protein expression of PTSD mice, and the distribution of armodafinil in vivo would be conducted to verify the anti-PTSD effect of AIC hydrogel.

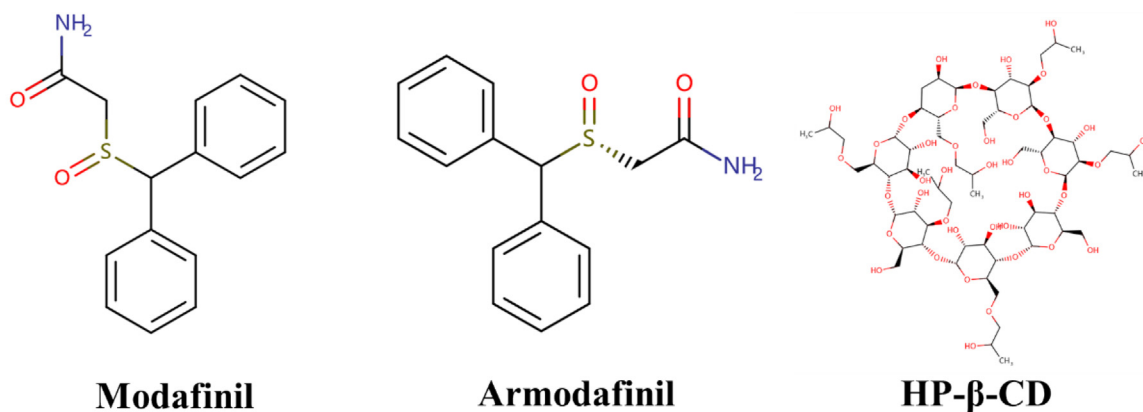


Fig. 1. Chemical structure of modafinil, armodafinil and HP- β -CD.

2. Materials and methods

2.1. Materials

Armodafinil was provided by the Institute of Radiation Medicine, Academy of Military Medical Sciences). HP- β -CD was purchased from Shijiazhuang Pharmaceutical Group Zhongqi Pharmaceutical Technology Co., Ltd.. Methylcellulose (MC) was purchased from Shanghai Aladdin Bio-Chem Technology Co., Ltd.. CORT enzyme immunoassay kit was purchased from Shanghai Lianmai Biotechnology Co., Ltd. Cy7 was provided by Beijing Fanbo Biochemicals Co., Ltd.. Isoflurane was purchased from Lunan Better Pharmaceutical Co., Ltd. Other solvents and reagents were of analytical grade or chromatographic reagents.

2.2. Animals

Healthy male C57 mice, weighing 18–20 g, were purchased from Beijing Vital River Laboratory Animal Technology Co., Ltd. with the license Number of SCXK (Beijing) 2016-0006. Animals were housed in separate cages in 12 h day-night alternating environment at 24–25 °C and (50 \pm 5)% humidity and were acclimatized for one week before the experiment was conducted. The animal welfare and experimentation program are reviewed and approved by the Beijing Institute of Radiation Medicine.

2.3. Measurement of armodafinil

Armodafinil was determined by HPLC (Agilent 1260, Agilent Technologies, USA) with the chromatographic column of Diamonsil C18 (5 μ m, 250 mm \times 4.6 mm). The mobile phase was water/acetonitrile (60:40, v/v) with temperature of 25 °C, detection wavelength of 225 nm, flow rate of 1 mL \cdot min $^{-1}$ and the injection volume of 10 μ L. Armodafinil was dissolved in the mobile phase to prepare samples of different concentration, 10, 50, 100, 200, 500, 1000 μ g \cdot mL $^{-1}$. Then they were filtered using the organic phase microporous membrane of 0.22 μ m and detected. The regression linear equation was established with concentration C (μ g \cdot mL $^{-1}$) as the horizontal coordinate and the peak area S (mAU \cdot s) as the vertical coordinate.

2.4. Molecular dynamic simulation and experimental verification for the optimal molar ratio of armodafinil and HP- β -CD

Materials Studio 7.0 (Accelrys Co., US) was used to simulate an experimental scenario, in which 10 mg of armodafinil in 10 mL water, and 1/3, 1/2, 1, 2, 3, and 4 times the armodafinil molar number of HP- β -CD was put into respectively, to carry out molecular dynamic simulation. In an amorphous chamber (26.9 \times 26.9 \times 26.9 Å^3), the kinetic system was constructed under the COMPASS force field. Then the average density ρ of armodafinil, HP- β -CD, and water at different molar ratio compositions was calculated by computer automatically.

Under the COMPASS force field in Materials Studio 7.0 (Accelrys Co., US), the initial configuration of the system was minimized in 10,000 steps, with an energy convergence threshold of 1×10^{-4} kcal \cdot mol $^{-1}$ and a force convergence value of 0.005 kcal \cdot mol $^{-1}\cdot$ Å $^{-1}$.

Then thermal annealing was performed at 1–300 K. The molecular dynamics equilibrium simulations were performed at 500 ps for each of the above six systems at an isothermal-isobaric pressure of 300 K (26.85 °C), and trajectory files were generated every 5 ps. The cohesive energy density was calculated from the data of the last five matched files.

In a real-life experiment, 10 mg of armodafinil was put into 10 mL water, and then 0.5, 1, 1.5, 2, 2.5, 3, 3.5 times of the

armodafinil molar number of HP- β -CD were put into the water, respectively. Then the mixers were thoroughly shaken for 24 h. The content of armodafinil in the corresponding solution was determined by HPLC, so as to determine the phase solubility.

2.5. Preparation and characterization of AIC by freeze-drying method

According to the above experimental results, armodafinil and HP- β -CD were used to prepare AIC at a 1:1 M ratio. 100 mg armodafinil was dissolved in 10 mL of methyl alcohol, ethyl alcohol, and tertiary butanol, separately, and mixed drop by drop with 10 mL HP- β -CD aqueous solution with the concentration of 56 mg/mL. After magnetically stirring for 15 min, it was placed in a –35 °C freeze dryer (LGJ-30F, Beijing Songyuan Huaxing Technology) to be lyophilized for 40 h. Finally, different kinds of AIC lyophilized in different solvents were obtained and recorded as sample A, B, and C, respectively.

Infrared spectroscopy (IR) (Spectrum Two, Perkin Elmer, US.) and differential scanning calorimetry (DSC) (Q200 TA Instrument-Waters LLC) measurements were performed on above sample A, B and C, respectively, by which the AIC formation was determined qualitatively. To be specific, the Fourier transform infrared spectrometer was set up according to the following parameters: test value as transmittance, variant trace method as Happ-Genzel, number of scans as 10, resolution as 4.0, and set the scan range as 600–4000 wave numbers. After the parameters were set up, an environmental scan minus background parameters was firstly performed and used as a reference. 10 mg of Sample A, B, C, Powder mixture (Armodafinil/HP- β -CD, 1:1), HP- β -CD, and Armodafinil were measured and placed in the pressure molds, flattened and pressed down to form a scannable tablet, and then placed on the spectrometer detection plate for scanning. Samples A, B, C, Powder mixture (Armodafinil/HP- β -CD, 1:1), HP- β -CD, and Armodafinil were respectively measured in 10 mg and sealed in an aluminum crucible, meanwhile, a blank aluminum crucible was sealed as a control. Then the differential scanning calorimetry analyzer was started with the rising temperature ranging from 40 to 330 °C, and the rising temperature rate was 10 °C/min, then the DSC curves of the above samples were measured.

In order to determine (encapsulation efficiency, EE) and (loading efficiency, LE) of the different lyophilized AIC, recorded as sample A, B and C. For each sample, two parts of AIC containing 100 mg armodafinil were precisely weighed. One part was dissolved in 20 mL of ultrapure water and filtered by 0.22 μ m aqueous microfiltration membrane. The total amount (W1) of armodafinil was measured by HPLC after 10 times dilution with methanol. The other part was dissolved in 20 mL of methanol, and filtered by a 0.22 μ m organic phase microporous membrane. The total amount (W2) of armodafinil was measured by HPLC after 10 times dilution with methanol. The amount of HP- β -CD used in the AIC preparation was W3. The EE and LE of sample A, B, and C were calculated by the formula (Bittencourt et al., 2019). To investigate the solubilization effect of AIC made from different solvents on Armodafinil in aqueous solution, 100 mg armodafinil was dissolved in 20 mL of ultrapure water and filtered by 0.22 μ m aqueous microfiltration membrane. The total amount (W4) of armodafinil was measured by HPLC after 10 times dilution with methanol. The improved solubilization of armodafinil in aqueous solution, which was influenced by AIC made from different solvents, was evaluated by dividing W4 with W1.

$$EE = W1/W2 \times 100\%$$

$$LE = W1/(W1 + W3) \times 100\%$$

(Each step was repeated three times, data of which were recorded as $\bar{x} \pm s$. \bar{x} represented the mean value of W1, W2 and W3 respectively, and the s represented the standard deviation.)

Molecular docking of armodafinil with methanol, ethanol, *tert*-butanol, and HP- β -CD was carried out through Sybyl 6.9.1 (Tripos, St. Louis, Missouri, US), respectively. Then intermolecular forces were calculated for each group to investigate the reason of different EE and LE in the process of AIC preparation in different solvents.

Based on the above experimental results, lyophilization of armodafinil dissolved in ethanol with the same number of moles of HP- β -CD in aqueous solution was determined to be the optimal method for the preparation of AIC.

Nasal perfusion method was used to compare the transmucosal efficiency of AIC and pure armodafinil. Internal catheter of the constant flow pump was flushed and filled with saline solution. The filled saline solution was drained into a graduated cylinder, and the fluid volume V_0 was recorded as a dead space volume of 1.4 mL. 0.1 mL of the sodium pentobarbital solution (1%, w/v) was used as anesthetic in the operation of intraperitoneal anesthesia. The C57 mouse was immobilized on the console, and the trachea was opened and exposed by a tracheal tube for ventilation. Internal catheter of the constant-flow pump was drained and attached with a butterfly needle that was inserted carefully through the esophagus against the epiglottis of the mouse.

The artificial nasal solution was prepared as follows. 7.91 g of sodium chloride, 3.68 g of potassium chloride and 0.51 g of calcium chloride were dissolved in deionized water of 1 L, sonicated for 1 min to obtain a clarified solution (Destruel et al., 2020). The AIC and armodafinil were added into the artificial nasal solution of 20 mL with the final concentration of 1 mg/mL. Both of the samples were added into the cylinder separately, where the total dose of armodafinil (Q) was 20 mg. Inserted the inlet tube of the constant-flow pump into the cylinder, aligned the nose of the mouse with the opening of the cylinder, added the magnetic stirring, and turned on the constant-flow pump for the experiment (Fig. 2).

The volume of circulating liquid V_t in the cylinder was recorded at every time t , 0.5 mL sample was taken out and fresh artificial nasal fluid of 0.5 mL was supplemented. The armodafinil concentration C_t was determined by HPLC after 10 times dilution with methanol. The nasal mucosa absorption dose Q_t was calculated as follows (Du et al., 2016):

$$Q_t = Q - [C_t \hat{A} \cdot (V_t + V_0) + 0.5] \hat{A} \cdot \sum_{i=1}^{t-1} c_i$$

(Each step was repeated three times, the nasal mucosa absorption dose Q_t was recorded as $\bar{x} \pm s$. \bar{x} represented the mean value, and the s represented the standard deviation.)

A linear fit was performed to each curve with time as the X-axis and Q_t as the Y-axis, which was took the first derivative to obtain the mucosal absorption rates of AIC and armodafinil, respectively.

2.6. Preparation and characterization of AIC hydrogel

A methylcellulose solution (3.3%, w/v) in water was chosen as the hydrogel matrix to load AIC because it could crosslink quickly in the range from 1.7% to 3.5% (w/v) (Niemczyk-Soczynska et al., 2019). Therefore, the AIC lyophilized powder was added to MC hydrogel to produce AIC hydrogel with the armodafinil content of 20 mg/mL and the MC mass fraction of 3.3% (Fig. 3).

2.6.1. Rheological investigation of AIC hydrogel

5 mL of blank MC hydrogel and AIC hydrogel were added to the plate of rheometer (HAAKE MARS60, Thermo Fisher Scientific), respectively. Since the ambient temperature of the nasal valve region is 34 °C and the oscillation frequency of the nasal cilia is 12–15 Hz (Gizurarson, 2015; Nishimura and Kaneko, 2019), the changes of energy storage modulus G' , loss modulus G'' and composite viscosity $|\eta^*|$ were investigated at the condition of 34 °C and 0–25 Hz shear frequency.

2.6.2. In-vitro drug release of AIC hydrogel

5 mL of armodafinil suspension, AIC aqueous solution and AIC hydrogel, containing 20 mg/mL of armodafinil respectively, were added into 5 cm-long dialysis bags with the cut-off MW of 3500, which were put into a 50 mL centrifuge tube subsequently. Then 30 mL of artificial nasal fluid was added to each centrifuge tube as the release medium. Considering the special temperature of nasal cavity and required frequency for in-vitro drug release, the released armodafinil was determined in the thermostatic air oscillator (THZ-D, Taicang Experimental Equipment) under 34 °C (Gizurarson, 2015; Nishimura and Kaneko, 2019) and 200 rpm (Swain et al., 2019; Pang et al., 2021). Detected the concentration of armodafinil outside the dialysis bag by taking 1 mL of dialysate from a centrifuge tube every 1 h, and promptly replenished 1 mL of artificial nasal solution. Each step was repeated three times with the data recorded as $\bar{x} \pm s$. The cumulative released percentage of armodafinil should be calculated according to the formula: (Q_n is the cumulative released percentage of armodafinil, V is the volume of the artificial nasal fluid, C_n and C_i are the concentration mea-

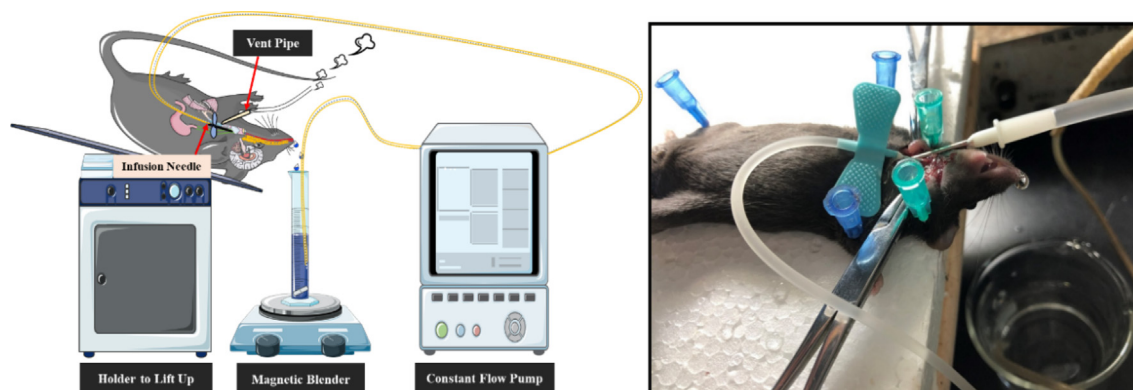


Fig. 2. Diagram of nasal mucosal irrigation experiment. (The C57 mouse was immobilized on the console, and the trachea was opened and exposed by a tracheal tube for ventilation. Internal catheter of the constant-flow pump was drained and attached with a butterfly needle that was inserted carefully through the esophagus against the epiglottis of the mouse. Armodafinil concentrations were measured at intervals of time t , and the absorbed dose and rate of nasal mucosa were calculated.)

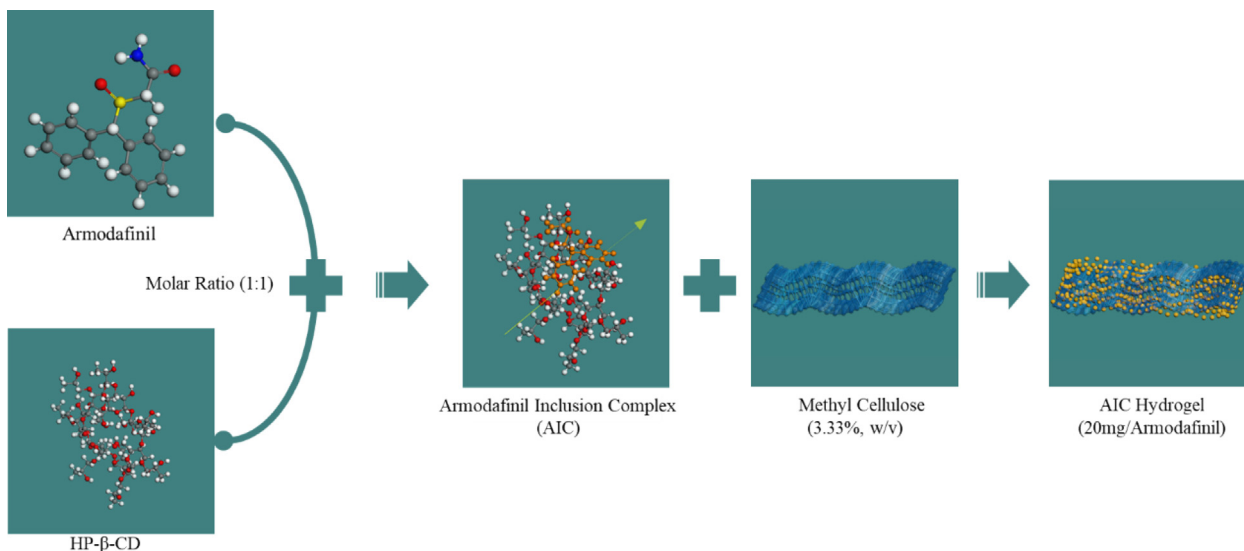


Fig. 3. Preparation illustration of AIC hydrogel. (Lyophilization of armodafinil dissolved in ethanol with the same number of moles of HP-β-CD in aqueous solution was used to prepare AIC. The AIC lyophilized powder was added to MC hydrogel to produce AIC hydrogel with the armodafinil content of 20 mg/mL.)

sured at the n th and i th sampling point, V_0 is the sampling volume, and A is the total amount of armodafinil in the two solutions. \bar{x} represented the mean value, and the s represented the standard deviation)

$$Q_n = \frac{C_n \cdot V + V_0 \sum_{i=1}^{n-1} C_i}{A} \times 100\%$$

A linear fit was performed to each curve with time as the X-axis and Q_n as the Y-axis, which was took the first derivative to obtain the release rates of armodafinil, AIC hydrogel, and AIC aqueous solution, respectively.

2.6.3. Mucosal irritation investigation of AIC hydrogel

Mucosal irritation experiment is commonly used to evaluate the safety of preparations (Chu et al., 2013; Takalkar and Desai, 2018). The mucosa of the upper jaw was separated after the execution of 5 toads. Then 15 pieces of mucosa with 5 mm × 5 mm each were divided equally into five groups as Saline group, 1% Sodium Deoxycholate group, AIC Aqueous Solution group, Blank Hydrogel group, and AIC Hydrogel group, immersing in five petri dishes containing 0.9% saline. The mucosal was then placed on the slide with cilia faced up, followed by the addition of 100 μL saline, 1% sodium deoxycholate, AIC aqueous solution containing Armodafinil 20 mg/mL, AIC hydrogel containing Armodafinil 20 mg/mL and 3.3% MC dropwise, respectively. Covered with cover glass, the samples were placed in petri dishes saturated with water vapor, and observed under a 200× microscope. The persistent vibration duration (PVD) of the cilia was recorded when the cilia stopped oscillating. The percentage of persistent vibration (PPV) was obtained by comparing the PVD of the cilia in the maxillary mucosa of each group with that of the cilia in the saline group. The higher the PPV, the less the toxicity of the drug to cilia.

2.7. Pharmacodynamics study of AIC hydrogel

2.7.1. Establishment of PTSD mice by inescapable foot shock and the treatment protocol

Fifty C57 mice were randomly divided into Healthy group, Model group, Sertraline group, AIC Hydrogel group and AIC Aqueous Solution group with 5 mice in each group after 7 days of acclimatization in the animal room. The fear-conditioning box in the size of 26 cm × 26 cm × 50 cm, which was equipped with

an electric grid for foot shock in the bottom used for the model establishment. The healthy mice were placed in the box for 600 s without any stimulation. Mice in the other four groups were subjected to inescapable foot shock to establish a PTSD model in the box (Louvar et al., 2005; Schöner et al., 2017). The procedure of model establishment was divided into two phases: a spontaneous activity phase in which the mice were free to move around in the fear-conditioning box for 300 s. In the subsequent electric shock stimulation phase, the mice experienced an inescapable foot shock with an intensity of 0.8 mA for 10 s, with an interval of 10 s. The cyclic process was repeated 15 times. Above operations were performed for 2 consecutive days, which were recorded as Day 1 and Day 2.

Due to different mounts of drug volume required for intragastric versus nasal administration in mice (Kumaki et al., 2017; Xiao et al., 2020). AIC aqueous solution with 2 mg/mL armodafinil and AIC hydrogel containing 20 mg/mL armodafinil and 3.33% (w/v) MC were prepared separately. Sertraline suspension (3 mg/mL) was prepared as the positive control with the dose of 30 mg/kg, which was calculated according to the maximum clinical dose of sertraline in PTSD patients (Nair and Jacob, 2016; Cooper et al., 2017; Li et al., 2017; Rauch et al., 2019). The drug was administered at 1 h after the PTSD model was established on Day 2. Each mouse in the Sertraline group, AIC Aqueous Solution group and AIC Hydrogel group was given 0.2 mL of sertraline suspension by gavage, 0.2 mL of AIC aqueous solution by gavage and 20 μL of AIC hydrogel unilaterally in the nasal cavity, respectively. From the Day 2 to Day 12, the different preparations were administered once daily for 11 consecutive days. No treatment was taken for the Healthy group and Model group (the experimental procedure is shown in Fig. 4).

2.7.2. Behavioral and molecular biology indicators

On Day 11, freezing response of mice with different treatments were tested. The above 25 mice were placed in a fear-conditioning box, then the activity trajectory, freezing time and total active distances were recorded for 5 min so that the severity of symptoms such as re-experiencing and intrusions could be evaluated (Bali and Jaggi, 2015). On Day 12, the mice were placed in a 50 cm × 50 cm × 50 cm open-field box (DB015, Beijing Zhishuduo-bao Biological Technology), with the square area of 25 cm × 25 cm at the bottom of the box as the center of thigmotaxis area of the

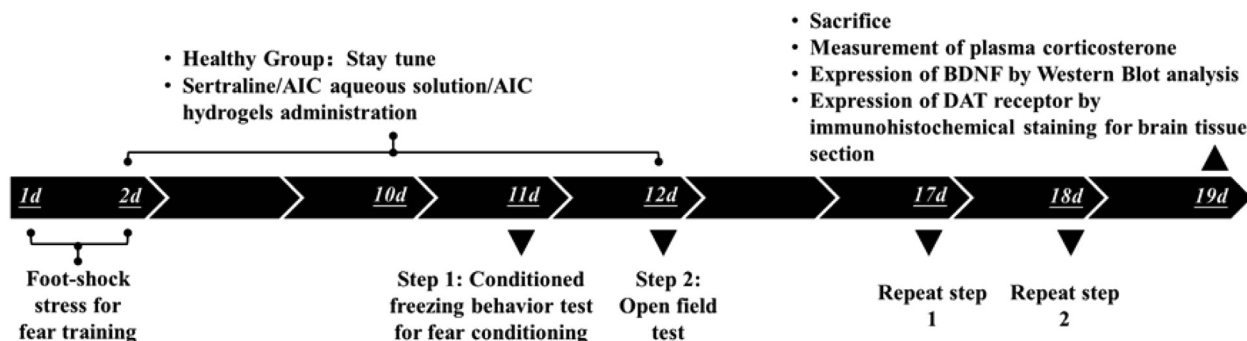


Fig. 4. The timeline of the pharmacodynamics study. (Day 1–2: placed the healthy mice in the box for 600 s without any stimulation. Mice in the other four groups were subjected to inescapable foot shock to establish a PTSD model in the fear-conditioning box. Day 2–12: Different preparations were administered once daily for 11 consecutive days. No treatment for the Healthy group and Model group. Day 11: Freezing response test. Day 12: open field test. Day 17: repeated freezing response test. Day 18: repeated open field test. Day 19: Determination of CORT, BDNF and DAT.)

open field and the rest of the box as the peripheral area. The trajectories of the mice within 5 min, the number of times they crossed the center of thigmotaxis area of the open field, the active distances within the center and the total active distances were recorded to evaluate the spontaneous mobility, exploratory behavior and stress level (Kuniishi et al., 2017). Five days after drug withdrawal, freezing response test in fear-conditioning box and the open field test were repeated on Day 17 and Day 18, respectively, to evaluate the lasting therapeutic effect of the treatment protocols. On Day 19, mice were anesthetized completely with 5% isoflurane in a gas-anesthesia machine. 200 μ L of blood was collected from posterior orbital venous plexus and centrifuged at 1800g for 15 min, and the upper layer of plasma was taken for CORT detection. Besides, the mouse brain was collected and cut alongside the cerebral falx after sacrifice. The hippocampus was taken out from the left hemisphere of the brain, which was tested by WB on BDNF, and the immunohistochemical section of the DAT in amygdala was conducted against the right hemisphere of the mouse. Both two experiments aimed to investigate the nutritional status of the brain and explore the mechanism of drug action (the experimental procedure is shown in Fig. 4).

2.8. Evaluation of intranasal administration and brain targeting effects of AIC hydrogel

2.8.1. In-vivo imaging test

Two parts of 2.0 mg Cy7 were weighed and one part was added 1 mL of ultrapure water to form an aqueous solution of 2 mg/mL of Cy7. Another part was added 1 mL of ultrapure water and 33 mg of MC, then stirred well to swell and form a Cy7 hydrogel with 20 mg/mL of Cy7 and 3.3% (w/v) MC. The hair on head and back of total nine C57 mice were shaved off 5 days before in-vivo imaging. They were divided into Blank group, Per Os (P.O.) group and Nasal groups with 3 mice in each group. The mice in the Blank group were without any operations. Mice in P.O. group were given 20 μ L Cy7 aqueous solution by gavage, and mice in Nasal group were given 20 μ L Cy7 hydrogel by intranasal administration. Mice in three groups were photographed at (0, 0.25, 0.5, 1, 1.5, and 2) h for in-vivo imaging (IVIS Lumina Series III, Perkin Elmer, Waltham, Massachusetts, US) after administration. According to the imaging shape, the region of interest (ROI) was marked with an ellipse on the minimum area of the imaging shape, and the average radiation efficiency, representing the imaging of three groups of mice, were calculated.

2.8.2. Pharmacokinetic evaluation

The pharmacokinetic evaluation of AIC hydrogel was conducted by liquid chromatography tandem mass spectrometry (LC-MS/MS)

(LC-20AD, Shimadzu, Japan; API5000, Applied Biosystems Sciex, USA). Acetaminophen was chosen as the internal standard, because of the similar amide group in their structures (Fig. 5).

The chromatographic conditions were: column: Kinetex C18 (3.0 mm \times 50 mm, 2.6 μ m, Phenomenex, USA); mobile phase A: 0.1% formic acid aqueous solution; mobile phase B: 0.1% formic acid acetonitrile solution; gradient elution: 0–0.5 min, 2% B; 0.5–1.8 min, 2–90% B; 1.8–2.4 min, 90% B; 2.4–2.5, 90–2% B; 2.5–4 min, 2% B; flow rate 0.7 mL/min; column temperature: 40 $^{\circ}$ C; injection volume: 5 μ L.

The mass spectrometry conditions were: the mass charge ratio (m/z) of armodafinil was 274.1 (Q1) for parent ion and 167.0 (Q3) for major fragment ion; the m/z of acetaminophen was 152.1 (Q1) for parent ion and 110.2 (Q3) for major fragment ion (Chandasana et al., 2018) (Table 1).

Eighteen C57BL/6N mice were randomly divided into Armodafinil group, AIC Aqueous Solution group, and AIC Hydrogel group. Each group consisted of 6 animals and was divided equally between males and females. Armodafinil suspension containing 2 mg/mL armodafinil with 0.5% mass fraction of sodium carboxymethylcellulose, AIC aqueous solution containing 2 mg/mL armodafinil and AIC hydrogel containing 20 mg/mL armodafinil with 3.33% MC were prepared, respectively.

0.2 mL of the corresponding solution was administered by gavage to each mouse in the Armodafinil and AIC Aqueous Solution groups, and 20 μ L of AIC Hydrogel was given through unilateral nasal cavity to each mouse in the AIC Hydrogel group. After administration, about 100 μ L of blood was collected from the posterior orbital plexus of mice at 5 min, 15 min, 30 min, 1 h, 2 h, 4 h, 6 h and 12 h. The blood was placed in a 1.5 mL centrifuge tube washed

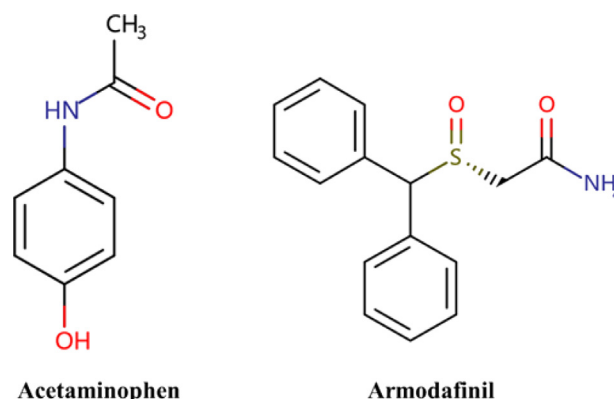


Fig. 5. Diagram of the structure of acetaminophen and armodafinil.

Table 1
Parameters of mass spectrometric analysis of armodafinil and acetaminophen.

Component	m/z		CE (V)	CXP (eV)	DP (eV)
	Q1	Q3			
Armodafinil	274.1	167.0	126	16	146
Acetaminophen	152.1	110.2	76	10	100

with sodium heparin and centrifuged at 4000 rpm for 10 min at 4 °C. The upper layer of plasma was carefully collected and stored at –80 °C in a refrigerator. In addition, blank plasma from unadministered mice was collected and stored by the above method.

A 30 ng/mL acetaminophen solution was prepared with acetonitrile as an internal standard. 100 µL of 5 ng/mL acetaminophen acetonitrile solution was used as responsive assessment.

Standard curve establishment: concentrations of (1000, 5000, 10,000, 20,000, 50,000, 100,000, 200,000, 500,000) ng/mL armodafinil solution was prepared with acetonitrile. 1 µL of above armodafinil solutions with different concentrations and 50 µL of the internal standard solution were added separately into 10 µL of blank plasma, and then mixed well in the vortex way, followed by centrifugation at 14000 rpm/min for 10 min at 4 °C. 5 µL of the supernatant was taken into the injection cannula, and then 95 µL of 50% acetonitrile solution was added, followed by placing the cannula into the liquid phase vial.

Sample processing: 10 µL of plasma from each blood sampling time was prepared, 1 µL of acetonitrile was added, then 50 µL of the internal standard solution was added and mixed in the vortex way. The methods of centrifugation and dilution were performed in the same way as above.

Double blank (DB) establishment: 1 µL of acetonitrile and 50 µL of acetonitrile were added into 10 µL of blank plasma and mix well in the way of vortex. The methods of centrifugation and dilution were performed in the same way as above.

Control blank (CB) establishment: 1 µL of acetonitrile and 50 µL of internal standard solution were added into 10 µL of blank plasma and mixed well in the vortex way. The methods of centrifugation and dilution were performed in the same way as above.

Quality control (QC) establishment: (200, 4000 and 40,000) ng/mL armodafinil-plasma samples were prepared as QC according to the above standard curve preparation method. Subsequently, the above samples were tested and analyzed.

2.8.3. In-vivo tissue distribution evaluation of AIC hydrogel

The in-vivo tissue distribution evaluation of AIC hydrogel was conducted by LC-MS/MS. Ninety C57BL/6N mice were randomly divided into Armodafinil Group, AIC Aqueous Solution Group, and AIC Hydrogel Group, of which each group included 15 males and 15 females. Armodafinil suspension, AIC aqueous solution and AIC hydrogel were prepared in the same way as above.

The Armodafinil group and the AIC Aqueous Solution group were each given 0.2 mL of the corresponding solution by gavage, and the AIC Hydrogel group was given 20 µL of AIC hydrogel unilaterally in the nasal cavity of each mouse. At 10 min, 30 min, 2 h, 6 h and 12 h, 3 male mice and 3 female mice were sacrificed in each group. The brain and liver were obtained, washed with saline and weighed after absorbing water with filter paper. Then the tissue homogenate was prepared by adding ultrapure water according to the mass ratio of tissue: water (1:4) using a handheld disperser. In addition, the tissue homogenates of brain and liver of unadministered mice were collected as blank homogenates by the above method.

A 50 ng/mL acetaminophen solution was prepared with acetonitrile as an internal standard. 100 µL of 5 ng/mL acetaminophen acetonitrile solution was used as responsive assessment.

Concentrations of (10, 20, 50, 100, 200, 500, 1000, 2000, 5000, 10,000, 50,000) ng/mL armodafinil solution was prepared with acetonitrile for the establishment of standard curve of brain tissue. Concentrations of (500, 1000, 2000, 5000, 10,000, 20,000, 25,000, 50,000, 100,000) ng/mL armodafinil solution was prepared with acetonitrile for the establishment of standard curve of liver tissue. 5 µL of above armodafinil solutions and 200 µL of the internal standard solution were added separately into 50 µL of blank homogenates of brains and livers separately. Then they were mixed well in the vortex way, followed by centrifugation at 14000 rpm/min for 10 min at 4 °C. 10 µL of the supernatant was taken into the injection cannula, and then 90 µL of 50% acetonitrile solution was added, followed by placing the cannula into the liquid phase vial.

Sample processing: 50 µL homogenates of brain and liver tissue from each sampling time was prepared, 5 µL of acetonitrile was added, then 200 µL of the internal standard solution was added and mixed in the vortex way. The methods of centrifugation and dilution were performed in the same way as above.

Double blank (DB) establishment: 5 µL of acetonitrile and 200 µL of acetonitrile were added into 50 µL of blank homogenates of brain and liver tissue separately and mix well in the way of vortex. The methods of centrifugation and dilution were performed in the same way as above.

Control blank (CB) establishment: 5 µL of acetonitrile and 200 µL of internal standard solution were added into 50 µL of blank homogenates of brain and liver tissue separately and mixed well in the vortex way. The methods of centrifugation and dilution were performed in the same way as above. Then, the above samples were tested and analyzed.

2.9. Statistical analysis

Statistical analysis of the data was performed using SPSS 18.0 software (International Business Machines Corporation, Armonk, New York, US). The data were analyzed by the repeated measures of ANOVA only in the evaluation of intranasal administration by in-vivo imaging test. One-way ANOVA was used to compare the remaining data between multiple groups, and the data were presented as mean ± standard deviation ($\bar{x} \pm s$), with $P < 0.05$ or $P < 0.01$ indicating the significant difference.

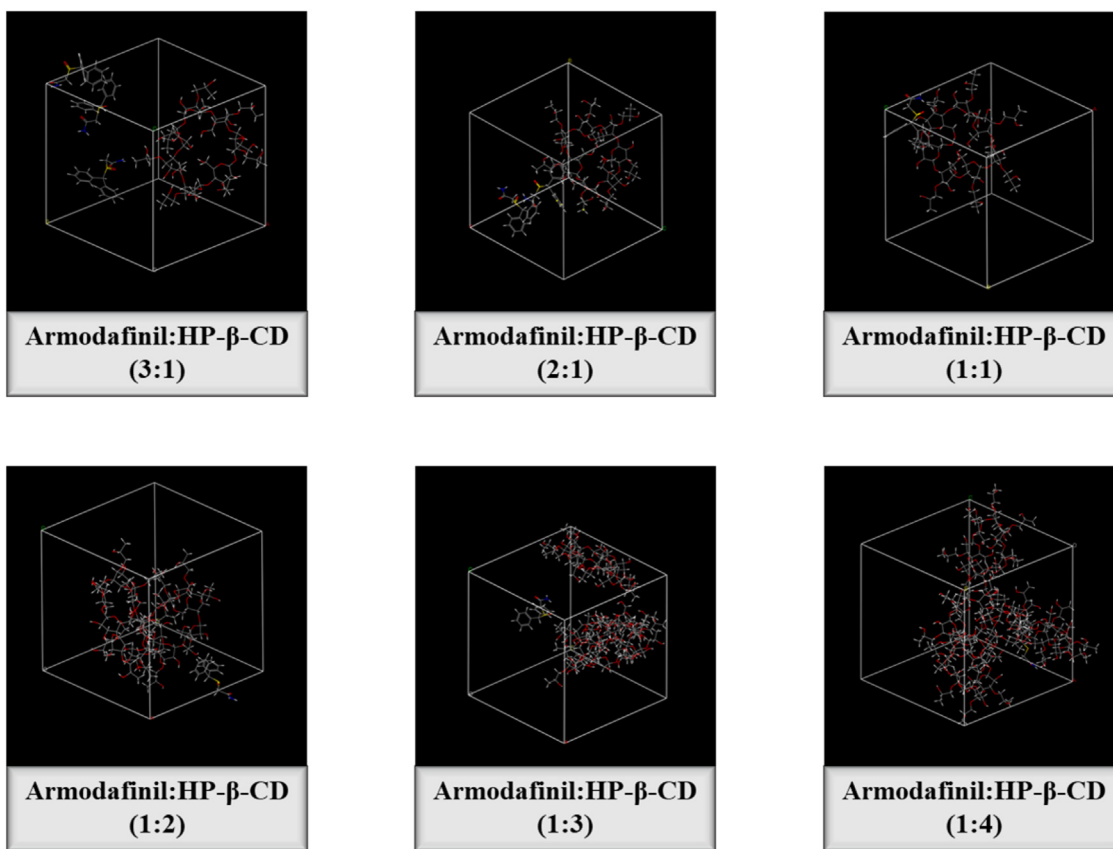
3. Results

3.1. The optimal ratio of armodafinil: HP-β-CD

Under the present chromatographic conditions in HPLC, there was a good linear relationship between peak area and drug concentration when the concentration of armodafinil ranged from 10 to 1000 µg·mL⁻¹. The regression equation is $S = 26.864C + 671.32$ ($r = 0.9957$).

In the simulated experimental scene, different molar ratio of armodafinil and HP-β-CD were put into 10 mL of water and the molecular dynamic simulation was conducted accordingly (Fig. 6A). The average density $\bar{\rho}$ and average cohesive energy density were then calculated (Table 2).

A



B

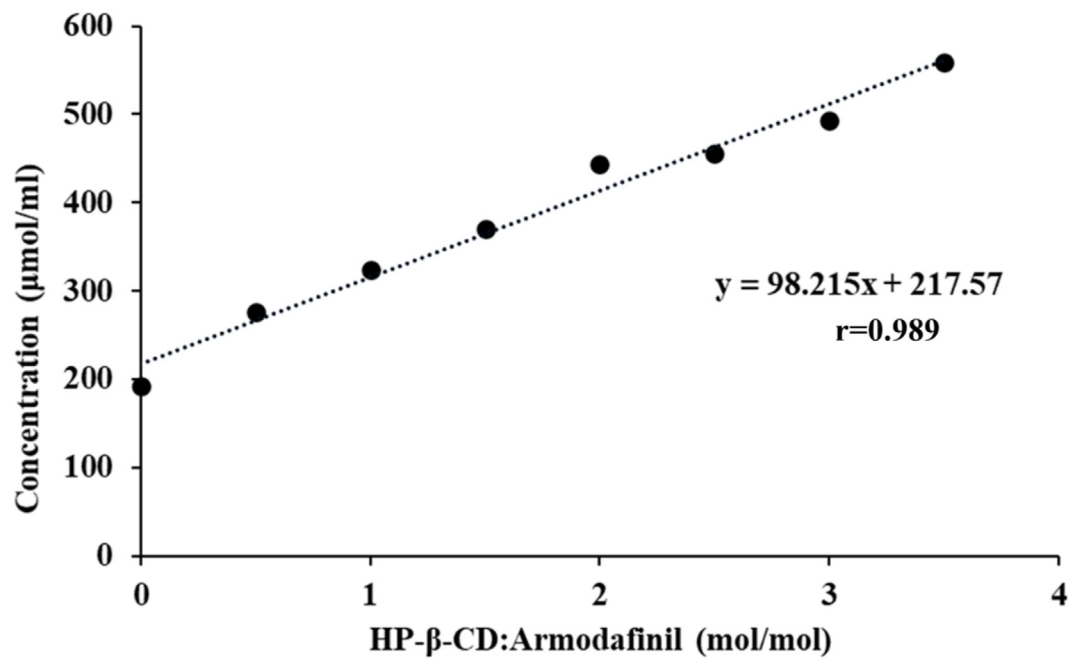


Table 2

Average density $\bar{\rho}$ and average cohesive energy density of armodafinil, HP- β -CD and water at different molar ratio compositions.

Component	Molar ratio	$\bar{\rho}$ (g·cm ⁻³)	Cohesive energy density ($\times 10^9$ Kcal·mol ⁻¹)
Armodafinil/HP- β -CD/H ₂ O	3/1/43100	1.00109	1.75 \pm 0.02
	2/1/30399	1.00130	1.80 \pm 0.05
	1/1/15200	1.00240	1.85 \pm 0.04
	1/2/15200	1.00468	1.68 \pm 0.03
	1/3/15200	1.00659	1.58 \pm 0.02
	1/4/15200	1.00896	1.49 \pm 0.03

(The value of cohesive energy density was maximum at 1:1 M ratio composition. The optimal input molar ratio for armodafinil and HP- β -CD to form an inclusion complex was 1:1.)

When the molar ratios of armodafinil and HP- β -CD were 3/1, 2/1, 1/1, 1/2, 1/3, and 1/4, the cohesive energy densities were (1.75 \pm 0.02) \times 109 kcal/mol, (1.80 \pm 0.05) \times 109 kcal/mol, (1.85 \pm 0.04) \times 109 kcal/mol, (1.68 \pm 0.03) \times 109 kcal/mol, (1.58 \pm 0.02) \times 109 kcal/mol, (1.49 \pm 0.03) \times 109 kcal/mol respectively. Therefore, the cohesive energy density was highest at a molar ratio of 1:1. The optimum input molar ratio for the formation of AIC was 1:1. In phase solubility experiments (Fig. 6B), the combination of armodafinil and HP- β -CD formed an AL-type phase solubility pattern, which provided a convincing evidence that the 1:1 M ratio of the armodafinil and HP- β -CD was a reasonable proportion for the preparation of AIC.

3.2. Characteristics of AIC

3.2.1. The prepared AIC was qualitatively verified by IR and DSC

Armodafinil was dissolved in methanol, ethanol and *tert*-butanol and mixed with HP- β -CD aqueous solution at a ratio of 1:1 molarity, and then lyophilized to produce AIC sample A, B and C (Fig. 7A). Sample A was homogeneous but not easy to scrape off the receptacle; sample B was homogeneous and easy to scrape; sample C was loose and easy to separate but has the pungent odor of *tert*-butanol.

The three samples were determined by IR. Armodafinil showed strong absorption peaks of carbonyl and sulfonyl groups near 1664 cm⁻¹ and 1029.58 cm⁻¹, respectively. Meanwhile, HP- β -CD showed middle absorption peaks of hydroxy and alkyl group near 3337.97 cm⁻¹ and 1331.31 cm⁻¹, respectively. Compared with armodafinil and the 1:1 M ratio of armodafinil/HP- β -CD physical mixture powder, the characteristic absorption peak of armodafinil in AIC of sample A, B, and C shifted from 1663 cm⁻¹ to 1677 cm⁻¹, and there was a blue shift of the carbonyl group, proving the formation of AIC (Fig. 7B).

DSC measurements showed that the melting temperature of armodafinil was 164 °C and the melting temperature of HP- β -CD was 267 °C. The 1:1 M ratio of armodafinil and HP- β -CD physically mixed powders produced two melting heat absorption peaks at 164 °C and 267 °C, respectively. The AIC in sample B and sample C melted to an amorphous state, demonstrating the formation of the inclusion. The AIC in sample A produces a heat-absorbing peak near 175 °C, which may be due to the co-fusion of a small amount of free armodafinil and the AIC (Fig. 7C).

3.2.2. High EE and LE of AIC and improved solubility

The EE and LE of lyophilized AIC sample A, B and C were determined. EE and LE of sample A were (81.62 \pm 5.84)% and (12.76 \pm 0.76)% respectively; EE and LE of sample B was (90.98 \pm 3.72)% and (13.95 \pm 0.47)% respectively, EE and LE of sample C was (92.39 \pm 4.06)% and (14.07 \pm 0.53)%. Therefore, the EE and LE of lyophilized AIC, made of armodafinil, dissolved in methyl alcohol, ethyl alcohol, and tertiary butanol respectively, and HP- β -CD aqueous solution at a 1:1 M ratio, increased sequentially. Compared with the raw armodafinil, AIC made with methyl alcohol, ethyl alcohol and tertiary butanol as solvents greatly increased the solubility of armodafinil in aqueous solution to 19, 21 and 21 times, separately.

To investigate the reasons for worse inclusion rate and loading of AIC prepared with methyl alcohol as solvent, armodafinil was molecularly docked with methyl alcohol, ethyl alcohol, tertiary butanol, and HP- β -CD, and the absolute intermolecular forces were 3.087 kcal/mol, 0.765 kcal/mol, 0.985 kcal/mol, and 2.522 kcal/mol, respectively (Fig. 8). The absolute value of the intermolecular force between armodafinil and methyl alcohol was greater than the absolute value of the intermolecular force between armodafinil and HP- β -CD, and solvent compounds were easily formed during freeze-drying, so the EE and LE of the AIC were low. Due to the pungent odor of tertiary butanol deriving from solvent residues in the AIC powder made from tertiary butanol, ethyl alcohol was chosen as the solvent to dissolve armodafinil and mix it with HP- β -CD aqueous solution at a molar ratio of 1:1 and then lyophilize the AIC for final preparation.

3.2.3. Improved penetration of armodafinil through nasal mucosa by AIC

The mucosal absorptive amount of armodafinil in AIC aqueous solution and armodafinil suspension were 10.58 mg and 2.50 mg at 60 min, respectively. The first-order functions for AIC and armodafinil were $Q_{t1} = 0.1495 t + 3.0808$ ($r = 0.874$) and $Q_{t2} = 0.0402 t - 0.1909$ ($r = 0.975$), respectively, which clearly did not fit the trend change of the curves because the r values were too far away from 1. Functions after performing the second-order fit are $Q_{t1} = 0.0043 t^2 + 0.4064 t + 0.9405$ ($r = 0.980$) and $Q_{t2} = 0.0004 t^2 + 0.0152 t + 0.0173$ ($r = 0.990$), where the r value was very close to 1. Therefore, it is assumed that the second-order fit could support the experiment. The mucosal absorption rate functions of AIC and armodafinil were obtained by taking the first derivative of the second-order functions: $Q'_{t1} = 0.0086 t + 0.4064$, $Q'_{t2} = 0.0008 t + 0.0152$. Took Q'_{t1} minus Q'_{t2} to get the equation $0.0078 t + 0.3912$, which is obviously always greater than 0 for $t > 0$. Therefore, it was concluded that the mucosal absorption rate of AIC was always higher than armodafinil, implying that AIC improved the penetration of armodafinil into the nasal mucosa (Fig. 9).

3.3. Characteristics of AIC hydrogel

3.3.1. Rheological investigation

AIC hydrogel, containing 20 mg/mL armodafinil and 3.3% (w/v) MC, and the blank hydrogel with 3.3% (w/v) MC were prepared. The changes in energy storage modulus G' , loss modulus G'' and complex viscosity $|\eta^*|$ were detected at the condition of 34 °C and 0–25 Hz shear frequency. Blank hydrogel and AIC hydrogel were

Fig. 6. (A) Diagram of molecular dynamic simulation and (B) armodafinil phase solubility curve. ((A) In the simulated experimental scene, different molar ratio, ranging from 1/3 to 4, of HP- β -CD and armodafinil were put into 10 mL of water. Kinetic systems and molecular dynamic simulation were conducted in the amorphous chamber (26.9 \times 26.9 \times 26.9 Å³), under the COMPASS force field. (B) The inclusion complex of armodafinil and HP- β -CD formed an AL-type phase solubility pattern, ration of which was at the 1:1 M ratio.)

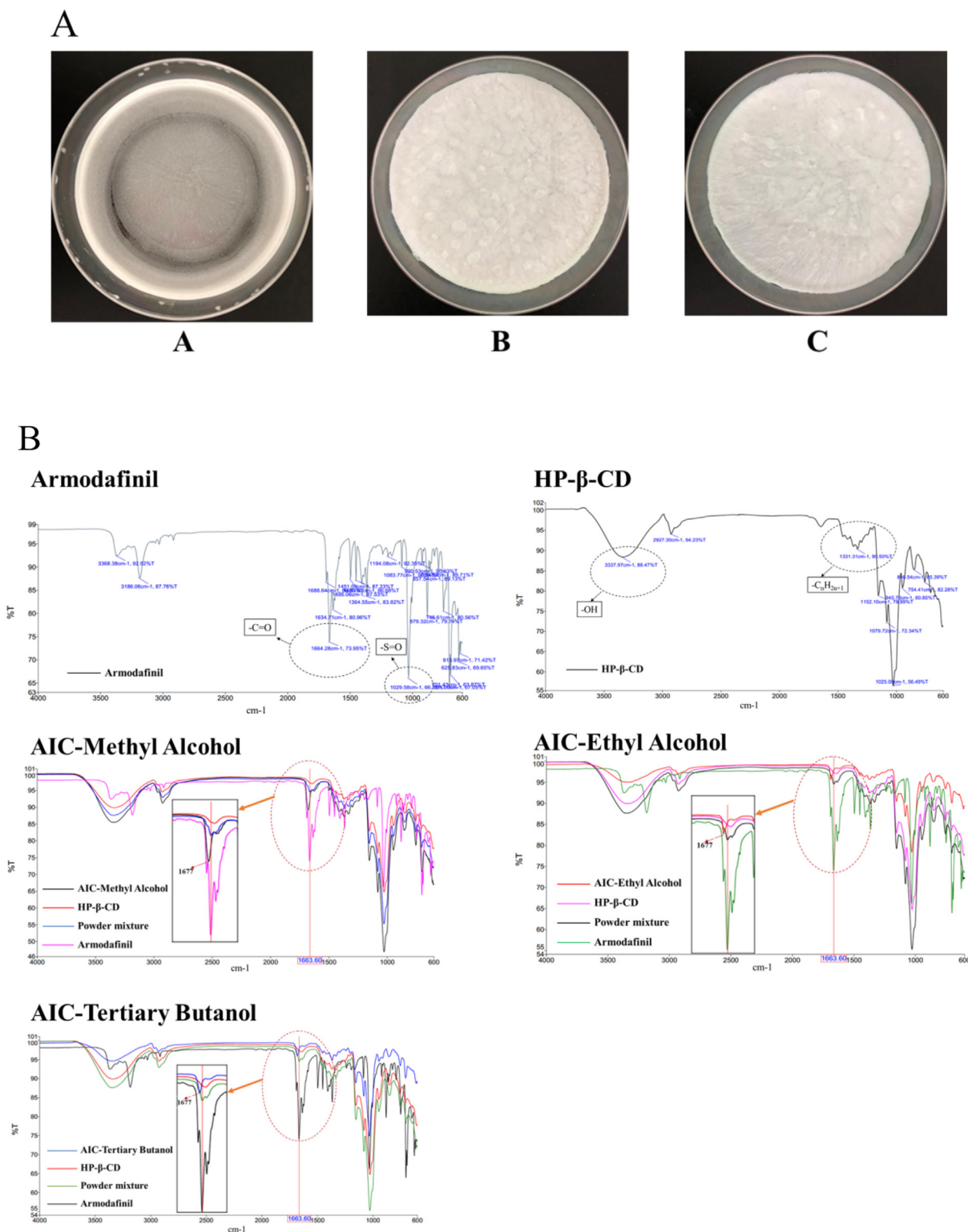


Fig. 7. (A) Appearance, (B) IR and (C) DSC of different AIC sample deriving from diverse preparation. ((A) A, B, and C samples were prepared by dissolving armodafinil with methanol, ethanol, and *tert*-butanol as solvents, and mixing it with HP-β-CD aqueous solution at a 1:1 M ratio and then lyophilizing to make the AIC. Sample A was homogeneous but not easy to scrape off the receptacle; sample B was homogeneous and easy to scrape; sample C was loose and easy to separate but has the pungent odor of *tert*-butanol. (B) Armodafinil and HP-β-CD represent the corresponding compounds, respectively. Powder Mixture represents a 1:1 M ratio physical mixture of armodafinil and HP-β-CD. AIC-Methyl Alcohol, AIC-Ethyl Alcohol, and AIC-Tertiary Butanol represent corresponding AIC produced by lyophilizing armodafinil with methanol, ethanol, and *tert*-butanol as solvents and mixing it with HP-β-CD aqueous solution at a ratio of 1:1 molarity. Compared with armodafinil, HP-β-CD and physical mixture powder, the characteristic absorption peak of armodafinil in AIC of sample A, B and C shifted from 1663 cm^{-1} to 1677 cm^{-1} , and there was a blue shift of the carbonyl group, proving the formation of AIC. (C) The melting process of AIC in AIC-Ethyl Alcohol and AIC-Tertiary Butanol, which was heated into an amorphous state is evidence of inclusion formation, while AIC in AIC-Methyl Alcohol produces a heat-absorbing peak near 175 °C, probably due to the co-fusion of small amounts of free armodafinil and AIC.)

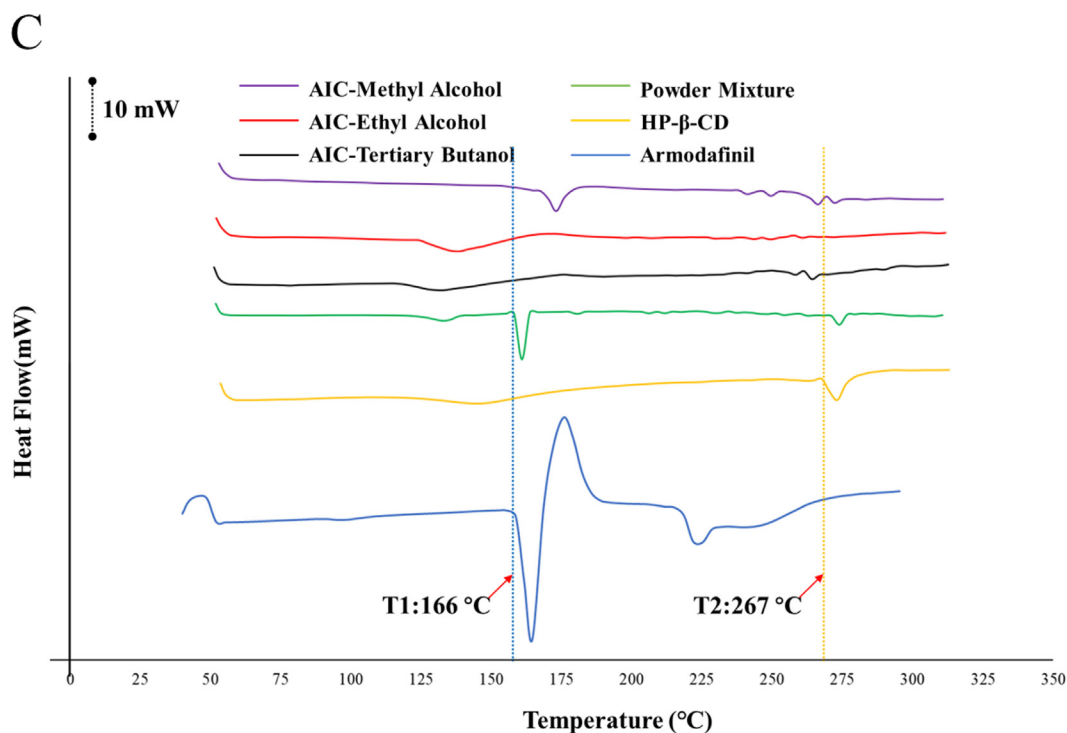


Fig. 7 (continued)

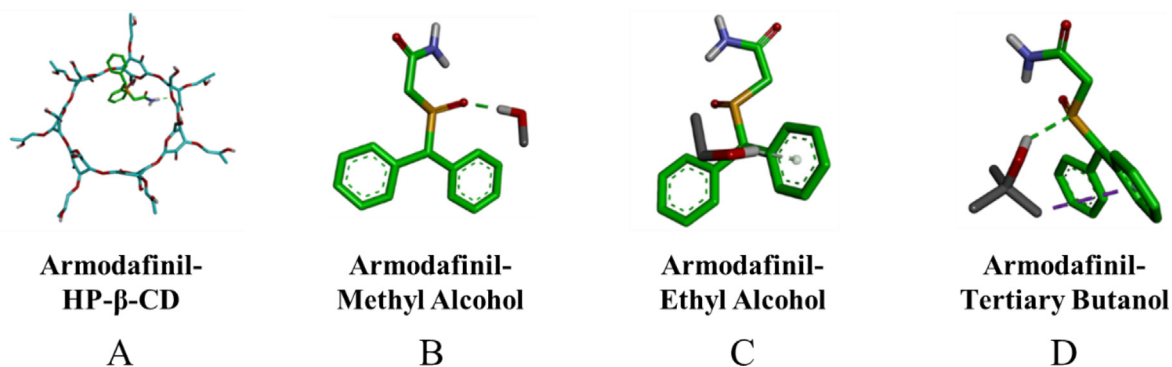


Fig. 8. Molecular docking of armodafinil to HP- β -CD (A), methyl alcohol (B), ethyl alcohol (C) and tertiary butanol (D). ((A) The bond between armodafinil and HP- β -CD is a hydrogen bond between the sulfinyl group and the hydroxyl group, and the absolute value of the intermolecular force is 2.522 kcal/mol. (B) The interaction between armodafinil and methyl alcohol is a hydrogen bond between a sulfinyl group and a hydroxyl group, with an absolute intermolecular force of 3.087 kcal/mol. (C) The interaction between armodafinil and ethyl alcohol is a large π -bond between the benzene ring and the alkyl group, with an absolute intermolecular force of 0.765 kcal/mol. (D) The bond with tertiary butanol is a combination of two bonds, the large π -bond between the benzene ring and the alkyl group, and a hydrogen bond between the sulfinyl group and the hydroxyl group, and the absolute intermolecular force is 0.985 kcal/mol. The absolute value of the intermolecular force between armodafinil and methyl alcohol is greater than the absolute value of the intermolecular force between armodafinil and HP- β -CD, which easily generates solvent compounds during freeze-drying, and contributes to a lower EE and LE.)

solid-like colloids with $G' > G''$ in the absence of shear. When shear frequency of blank hydrogel and AIC hydrogel reached 0.4 Hz and 0.8 Hz, respectively, $G' > G''$, at which the gel point was reached. Thereafter, as the shear frequency increased, $G'' > G'$, the gel turned into a viscous liquid, thus facilitating storage and providing good through-needle properties for usage. $|\eta^*|$ of both gels decreased with shear frequency increasing, showing a shear-thinning flow state, which was in accordance with the pseudoplastic flow rule, and thus the AIC hydrogel and blank hydrogel were fit into pseudoplastic fluid. Compared with blank hydrogel, G' , G'' , and $|\eta^*|$ of AIC hydrogel were larger owing to the exist of AIC aqueous solution in the hydrogel system (Fig. 10A).

3.3.2. AIC hydrogel is characterized to release higher percentage of armodafinil with a slow-release rate

Through graphing t by Q_n , the release of AIC hydrogel was complete at the 12th hour, the released armodafinil percentage was $(77.62 \pm 0.68)\%$. The release of AIC Aqueous Solution was complete at the 2nd hour, the released armodafinil percentage was $(79.66 \pm 0.26)\%$. The release of armodafinil suspension was complete at the 2nd hour, the released armodafinil percentage was $(18.12 \pm 1.03)\%$ (Fig. 10B). The three curves of Armodafinil, AIC Hydrogel and AIC Aqueous Solution were linearly fitted. Since both the Armodafinil curve and the AIC Aqueous Solution curve did not change significantly after 2 h, the curves before 2 h were took for the linear fit-

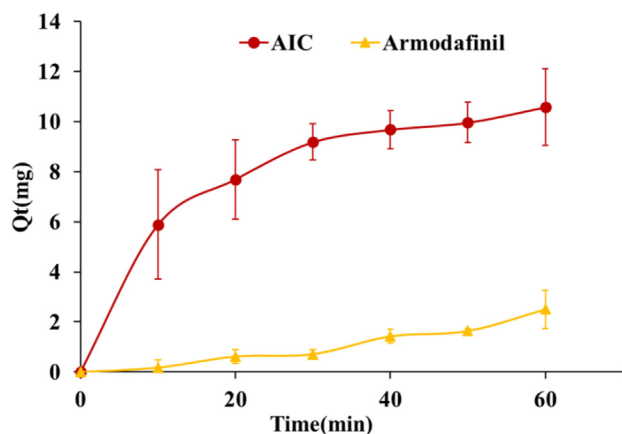


Fig. 9. Investigation of nasal mucosal penetration in mice by AIC and armodafinil. (The mucosal absorptive amount of AIC and armodafinil were 10.58 mg and 2.50 mg at 60 min, respectively; the mucosal absorption rate of AIC was always higher than that of armodafinil, implying that AIC improved the penetration of armodafinil into the nasal mucosa.)

ting process. Due to the imprecise first-order fit, the second-order fit was applied to get the functions for armodafinil, AIC hydrogel, and AIC aqueous solution, respectively: $Q_{n1} = -4.9941 t^2 + 17.517 t$ ($r = 1.000$), $Q_{n2} = -0.7091 t^2 + 13.054 t + 20.227$ ($r = 0.922$), and $Q_{n3} = -33.268 t^2 + 102.78 t$ ($r = 1.000$). The release rate functions of armodafinil, AIC hydrogel and AIC aqueous solution were obtained by taking the first derivative of the second-order functions, respectively: $Q'_{n1} = -9.9882 t + 17.517$, $Q'_{n2} = -1.4182 t + 13.054$, and $Q'_{n3} = -66.536 t + 102.78$. Since the release of armodafinil was completed and low at the 2nd hour, the release rate functions of AIC hydrogel and AIC aqueous solution were compared by subtracting Q'_{n3} from Q'_{n2} ($Q'_{n2} - Q'_{n3} = 65.1178 t - 89.726$). It is obviously that Q'_{n2} is always smaller than Q'_{n3} for $t < 1.4$, indicating that the release rate of AIC hydrogel was lower than AIC aqueous solution within 1.4 h. Due to the completed release of AIC aqueous solution at the 2nd hour, it was reasonable that the release rate of the AIC hydrogel was gradually higher than that of the AIC aqueous solution after 1.4 h. It was concluded that AIC hydrogel not only released relatively large, but also had a slower release rate in the release process.

3.3.3. AIC hydrogel is characterized as a safe preparation

The ciliary structure of the maxillary mucosa was observed by $400 \times$ microscope. The cilia in the Saline group oscillated rhythmically with neat anatomical structure and distinguished from basal cells. In the Sodium Deoxycholate group, the ciliary cells were obviously prostrate or even exfoliated. The boundary between ciliary and basal cells was blurred, and the anatomical structure was obviously damaged. The extent of damage of cilia in the AIC Aqueous Solution, Blank Hydrogel and AIC Hydrogel groups was slightly worse than that in the Saline group, but much better than that in the Sodium Deoxycholate group (Fig. 11). The PVD and PPV of the different groups were ranked in descending order: Saline group > AIC Aqueous Solution group > Blank Hydrogel group > AIC Hydrogel group > Sodium Deoxycholate group. There was a significant decrease in PVD and PPV in the Sodium Deoxycholate group compared with the Saline group. In contrast, the PVD and PPV in the AIC Aqueous Solution, Blank Hydrogel and AIC Hydrogel groups were not significantly different in value from those in the Saline group, respectively (Table 3). Therefore, AIC Hydrogel was relatively safe and could be used for intranasal administration.

3.4. High anti-PTSD efficiency of AIC hydrogel

In the freezing response test in fear-conditioning box on Day 11, mice in the Model group had a longer freezing time ($**P < 0.01$) and a shorter total active distances ($**P < 0.01$) compared to the Healthy group, which proved that the PTSD model of mice was established successfully by the inescapable foot shock method in the fear-conditioning box. Compared with Model group, Sertraline group, AIC Aqueous Solution group and AIC hydrogel group had shorter freezing time ($**P < 0.01$) and longer total active distances ($**P < 0.01$), which proved that the three therapeutic agents could alleviate PTSD symptoms in mice. Compared with Healthy group, Sertraline group and AIC Aqueous Solution group had longer freezing time ($**P < 0.01$) and shorter total active distances ($**P < 0.01$). More importantly, there were no significant differences between Healthy group and AIC Hydrogel group in terms of freezing time, which demonstrated that AIC hydrogel had a better effect on the re-experiencing of trauma in PTSD mice (Fig. 12A).

In the open field test on Day 12, compared with the Healthy group, the crossing times, the active distances in the center of thig-

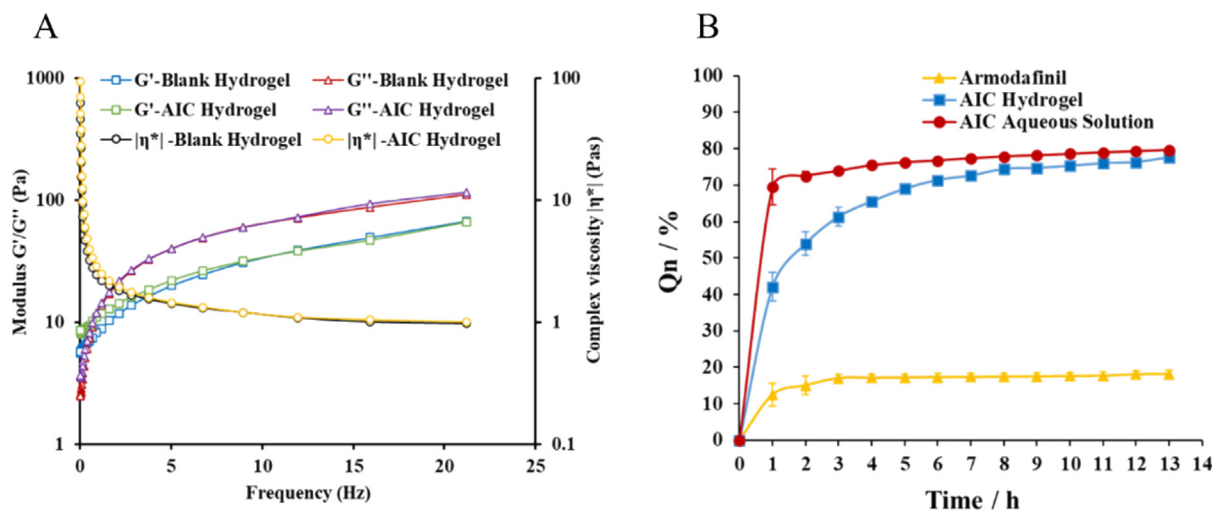


Fig. 10. Rheological investigation (A) and release curves in-vitro (B). ((A) G' is the energy storage modulus, G'' is the loss modulus, and $|\eta^*|$ is the complex viscosity. The AIC hydrogel and blank hydrogel were fit into pseudoplastic fluid. (B) AIC hydrogel and AIC aqueous solution released more completely at $(77.62 \pm 0.68)\%$ and $(79.66 \pm 0.26)\%$ respectively. AIC hydrogel had a slower release rate during the release process.)

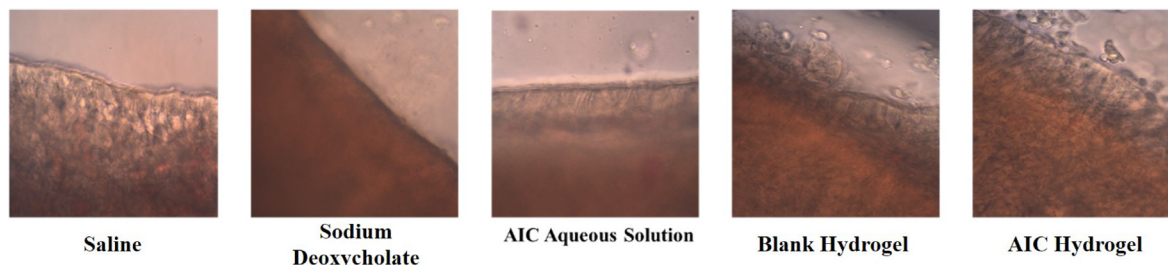


Fig. 11. Effect of AIC hydrogel on the structure of cilia in the maxillary mucosa of toads.

Table 3

Persistent vibration duration of mucosal cilia in the upper jaw of the toad.

Group	PVD(min)	PPV(%)
Saline	660.67 ± 25.38 ^{##}	100
Sodium Deoxycholate	136.67 ± 26.95 ^{**}	20.69
AIC Aqueous Solution	617.33 ± 13.05 ^{##}	93.44
Blank Hydrogel	605.33 ± 18.15 ^{##}	91.62
AIC Hydrogel	577.67 ± 18.72 ^{##}	87.44

[#]denotes statistical significance compared with the Sodium Deoxycholate group, ^{*}denotes statistical significance compared with the Saline group. ^{*} $P < 0.05$, ^{**} $P < 0.05$; ^{##} $P < 0.01$, ^{**} $P < 0.01$.

motaxis area and the total active distances decreased in the Model group (^{**} $P < 0.01$), which demonstrated the decrease in spontaneous activity and the increase in tension in the Model group. Mice in Sertraline, AIC Aqueous Solution and AIC Hydrogel groups had more crossings in the center of thigmotaxis area (^{##} $P < 0.01$), more active distances in the center of thigmotaxis area (^{##} $P < 0.01$) and more total active distances (^{##} $P < 0.01$) than the Model group. Compared with the Healthy group, the Sertraline group had fewer crossing times. There were no significant differences between Healthy group, AIC Aqueous Solution group and AIC Hydrogel group, which proved that armodafinil had a good effect on the anxiety symptoms of PTSD mice (Fig. 12B).

The freezing response test was carried out repeatedly five days after drug withdrawal. The freeing time was longer (^{**} $P < 0.01$) and the total active distances was shorter (^{**} $P < 0.01$) in the Model group compared with the Healthy group, as shown in the freezing response test in fear-conditioning box on Day 17. Compared with Model group, mice in Sertraline, AIC Aqueous Solution, and AIC Hydrogel groups all had shorter freezing time (^{##} $P < 0.01$) and longer total active distances (^{##} $P < 0.01$). Compared with Healthy group, the Sertraline and the AIC Aqueous Solution group had longer freezing time (^{*} $P < 0.05$, ^{**} $P < 0.01$) and shorter total active distances (^{*} $P < 0.05$, ^{**} $P < 0.01$). There were no significant differences in freezing time and total active distances between the Healthy group and AIC Hydrogel group (Fig. 12C).

Open field test was conducted again six days after drug withdrawal, the number of crossings times in the center of thigmotaxis area, the active distances in the center of thigmotaxis area and the total active distance decreased in the Model group (^{**} $P < 0.01$) compared with the Healthy group, as shown in the open field test on Day 18. Mice in Sertraline, AIC Aqueous Solution and AIC Hydrogel groups crossed the center of thigmotaxis area more frequently (^{##} $P < 0.01$) than those in Model group, AIC Hydrogel group had longer active distances in the center of thigmotaxis area (^{##} $P < 0.01$), besides the total active distances of Sertraline, AIC Aqueous Solution and AIC Hydrogel groups increased (^{##} $P < 0.01$). Compared with Healthy group, Sertraline, AIC Aqueous Solution, and AIC Hydrogel groups had fewer crossings and active distances in the center of thigmotaxis area (^{**} $P < 0.01$), Sertraline and AIC Aqueous Solution groups had fewer total active dis-

tances covered (^{**} $P < 0.01$). Encouragingly, there were no significant differences in the total active distances between Healthy group and AIC Hydrogel group (Fig. 12D).

In conclusion, AIC hydrogel has a good alleviating effect on the symptoms of trauma re-experiencing in mice at the early stage of PTSD. Sertraline, AIC Hydrogel and AIC Aqueous Solution have alleviating effects on the anxiety symptoms in PTSD mice, but among the specific indicators reflecting the effectiveness of the treatment, AIC hydrogel had better result in the treatment of PTSD, both in terms of statistical differences and comparison of mean value.

3.5. Regulation of HPA axis by AIC hydrogel

Plasma CORT levels in Healthy, Model, Sertraline, AIC Hydrogel, and AIC Aqueous Solution groups were measured separately on Day 19. Compared with Healthy group, the plasma CORT level in Model group (^{**} $P < 0.01$) and in Sertraline group (^{*} $P < 0.05$) were decreased and the HPA axis function was impaired; compared with Model group, the plasma CORT level in AIC Hydrogel and AIC Aqueous Solution groups was increased (^{##} $P < 0.01$), and there was no statistically significant difference with Healthy group. AIC hydrogel was shown to have a modulating effect on the HPA axis in PTSD mice, and the effect was the same as that of AIC Aqueous Solution (Fig. 13A).

3.6. Improved BDNF level in hippocampus and suppression of DAT expression in amygdala by AIC hydrogel

WB results showed that BDNF expression was decreased in the hippocampus of mice in the Model and Sertraline groups compared with the Healthy group (^{*} $P < 0.05$). BDNF expression was increased in the hippocampus of mice in the Healthy, AIC Hydrogel and AIC Aqueous Solution groups compared to the Model group ([#] $P < 0.05$). There was no statistically significant difference in BDNF expression among Healthy, AIC Hydrogel, and AIC Aqueous Solution group. It was demonstrated that AIC Hydrogel and AIC Aqueous Solution had good protective effects on the nervous system of mice (Fig. 13B). Immunohistochemical sections were observed under a 40 × microscope, which were analyzed using Image-Pro Plus software to calculate the integrated option density (IOD) of DAT expression regions. DAT expression was significantly increased in Model, Sertraline and AIC Aqueous Solution groups compared with the Healthy group (^{**} $P < 0.01$), and DAT expression was significantly decreased in Healthy, AIC Hydrogel and AIC Aqueous Solution groups compared with the Model group (^{**} $P < 0.01$). expression significantly decreased (^{##} $P < 0.01$) and there was no difference in DAT expression between the Healthy and AIC Hydrogel groups, demonstrating that AIC hydrogel alleviated the reward disorder in PTSD mice by specifically blocking DAT receptors and regulating dopaminergic neural pathways to achieve the therapeutic effect of the disease (Fig. 13C).

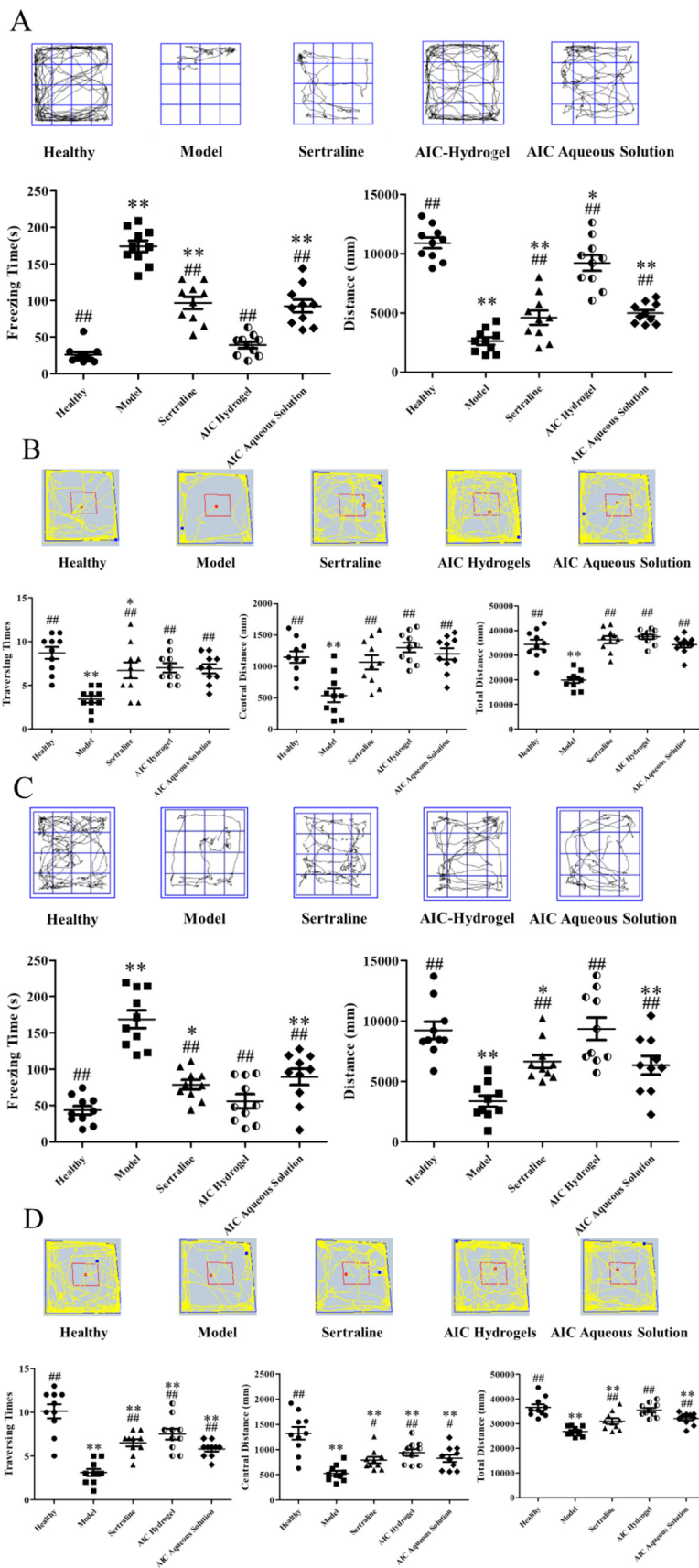


Fig. 12. Behavioral evaluation of the therapeutic effects of AIC hydrogel in PTSD mice. ((A) and (C) showed the freezing behavior test in fear-conditioning test on Day 11 and Day 17 after 5 days of drug withdrawal, respectively. (B) and (D) showed the open filed test on Day 12 and Day 18 after 5 days after drug withdrawal, respectively. # denotes statistical significance compared with the Model group, * denotes statistical significance compared with the Healthy group. ##*P* < 0.05, ***P* < 0.05; ###*P* < 0.01, ****P* < 0.01.)

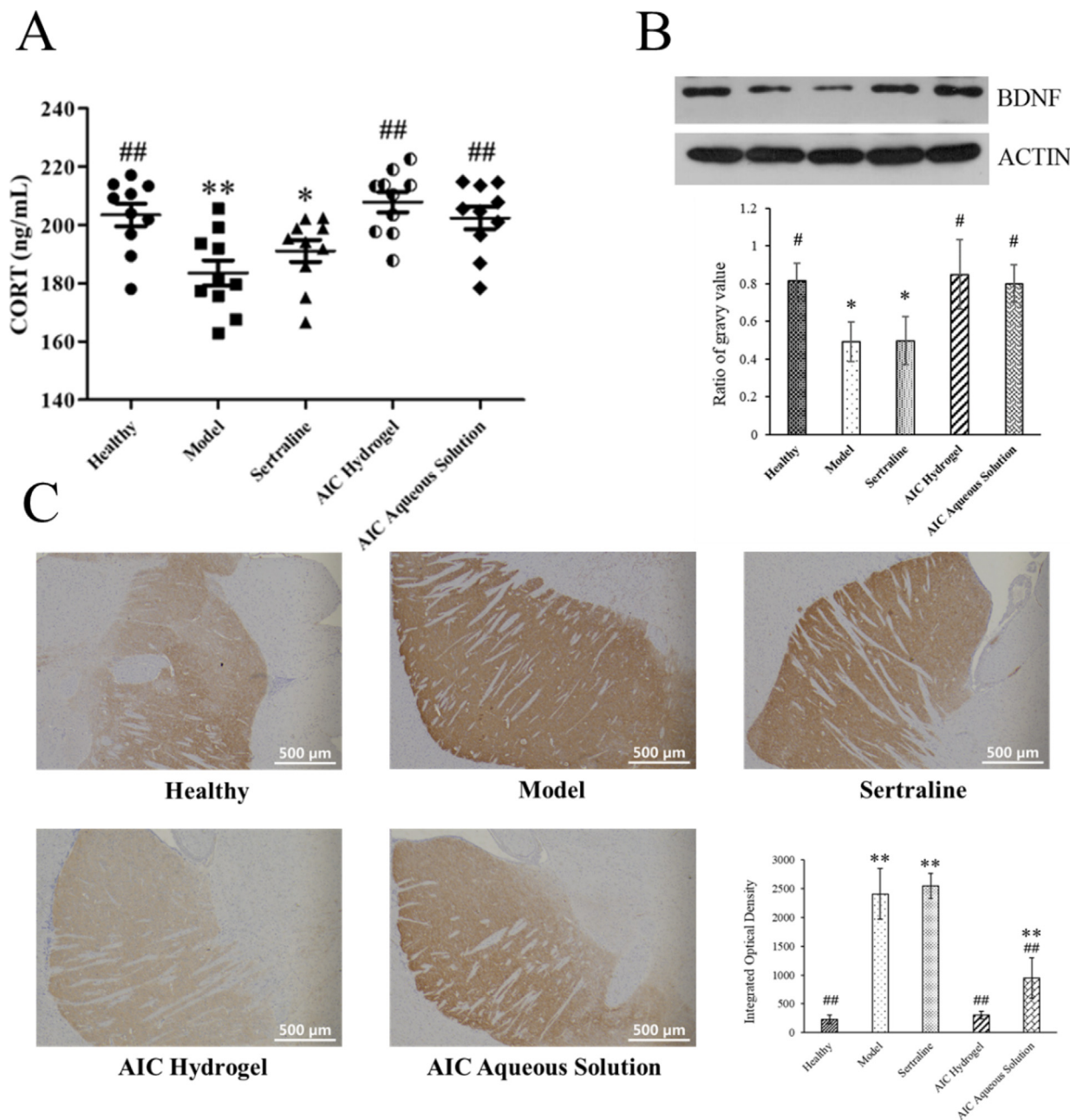


Fig. 13. AIC hydrogel regulates HPA axis, promotes BDNF elevation and suppresses DAT expression in PTSD mice. ((A) On Day 19, the above mice were completely anesthetized with 5% isoflurane, and 200 μ L of blood was collected for CORT test. AIC hydrogel increased the plasma CORT level in PTSD mice. (B) WB was used to detect the expression of BDNF in the hippocampus after sacrificing. AIC hydrogel increased the expression of BDNF in the hippocampus of PTSD mice. (C) Immunohistochemical sections of the amygdala were observed under a 40x microscope, calculating the integrated optical density (IOD) of the DAT-expressing region with x40 field of vision. AIC hydrogel suppressed DAT expression in amygdala of PTSD mice # indicates statistically significant compared with the Model group, and * indicates statistically significant compared with the Healthy group. * $P < 0.05$, ** $P < 0.05$, ## $P < 0.01$, ### $P < 0.01$).

3.7. Improved brain targeting by intranasal administration method and AIC hydrogel

The average radiative efficiency of ROI-Blank, ROI-P.O., and ROI-Nasal of the three groups of mice imaged is shown (Fig. 14). The ROI-Blank value was constant at zero, while the ROI-P.O. value reached a maximum value of 2.89×10^8 at 15 min and then remained constant, with the ROI region concentrated in the stomach of the mice. The average radiative efficiency of ROI-Nasal increased slowly to 6.83×10^8 within (0–2) h with the region concentrated in the head of mice. Therefore, the hydrogel intranasal administration method is characterized by slow drug release and

brain targeting enrichment. The average radiation efficiency of ROI-Nasal was greater than that of ROI-P.O. (* $P < 0.05$) within (0.5–2) h. The lower average radiation efficiency of ROI-P.O. should be due to the dilution of the drug by gastric acid in the stomach. Compared with oral absorption, intranasal administration of the drug has the characteristic of forming high concentrations locally with the same dosage and has a better osmotic potential of the drug.

The standard curve of armodafinil in blank plasma was evaluated. The actual concentration obtained from different amounts of armodafinil input was used as the horizontal coordinate x, and the measured amount of armodafinil by was used as the vertical

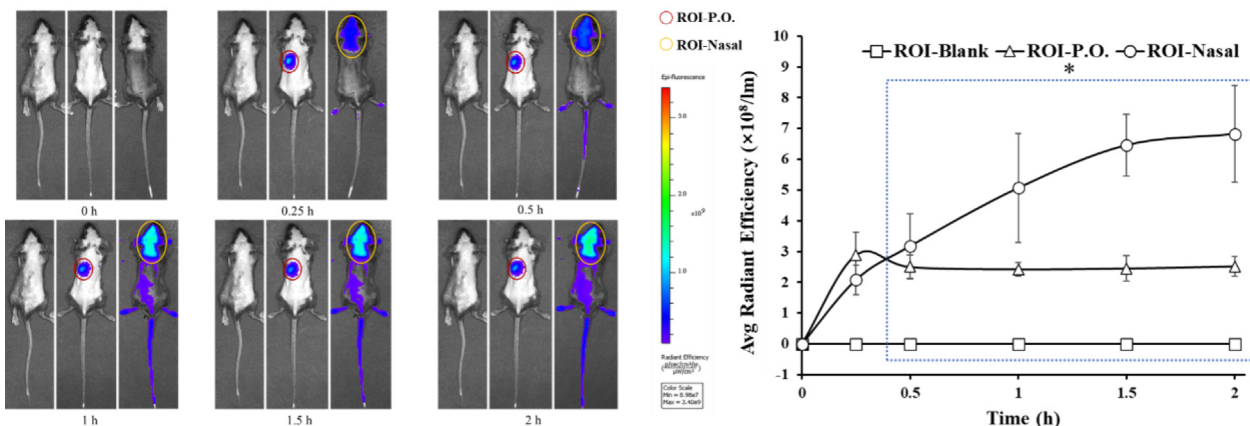


Fig. 14. In-vivo imaging of small animals to explore the advantages and characteristics of hydrogel intranasal administration. (Average radiation efficiency value in Blank group was constant at zero. The average radiation efficiency value of ROI-P.O. reached a maximum value of 2.89×10^8 at 15 min and then remained constant in the stomach. The average radiative efficiency of ROI-nasal slowly increased to 6.83×10^8 within 2 h with the concentrated region in the brain. ANOVA with repeated measurements indicated that, at (0.5–2) h, the average radiative efficiency of ROI-Nasal was greater than that of ROI-P.O. (* $P < 0.05$).

Table 4

Plasma pharmacokinetic parameters in mice (n = 6).

Parameter	Group		
	Armodafinil	AIC Aqueous Solution	AIC Hydrogel
Tmax (h)	0.25 ± 0.00	0.11 ± 0.07	0.5 ± 0.27
Cmax (ng/mL)	3597.09 ± 2251.00	11532.83 ± 2327.24	9927.97 ± 1859.16
AUClast (h ng/mL)	9901.12 ± 5498.48	20012.50 ± 6205.94	27150.83 ± 6926.25

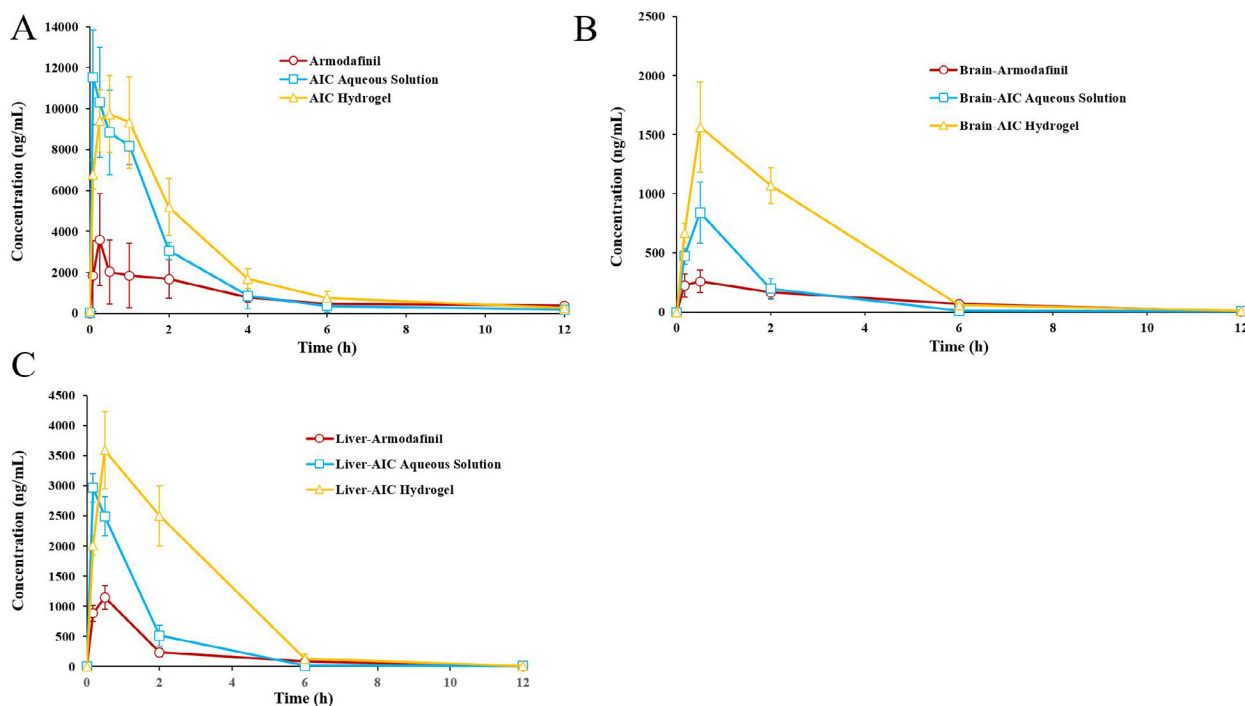


Fig. 15. Drug-time curve of armodafinil in the plasma (A), brain tissue (B) and liver tissue (C) of mice.

coordinate y. The linearity of Armodafinil concentration in plasma was investigated. The standard curve of mouse plasma sample was $y = 1.0392x - 7.749$ ($r = 0.999$), which had a good linear relationship.

From the pharmacokinetic parameters (Table 4) and the drug-time curves (Fig. 15A), the time of the concentration peak (Tmax) of armodafinil ingredient in raw armodafinil, AIC aqueous solution and AIC hydrogel in mice were 0.25 h, 0.11 h and 0.5 h, respec-

Table 5
Tissue distribution parameters in mice (n = 6).

Tissue	Group	Parameter		
		Tmax (h)	Cmax (ng/ml)	AUClast (h ng/ml)
Brain	Armodafinil	0.50	258.78 ± 95.97	1090.76
	AIC Aqueous Solution	0.50	841.89 ± 259.42	1501.47
	AIC Hydrogel	0.50	1565.03 ± 381.24	4861.25
Liver	Armodafinil	0.50	1151.18 ± 198.66	2378.63
	AIC Aqueous Solution	0.17	2966.91 ± 233.16	4568.03
	AIC Hydrogel	0.50	3590.17 ± 641.17	11352.08

tively. The maximum concentrations (Cmax) of armodafinil ingredient of three preparations in blood were 3597.09 ng/mL, 11532.83 ng/mL, 9927.97 ng/mL, and the area under the drug-time curve (AUClast) were 9901.12 h ng/mL, 20012.50 h ng/mL, and 27150.83 h ng/mL, respectively. Compared to raw armodafinil gavage, AIC aqueous solution gavage and AIC hydrogel nasal administration substantially increased the Cmax and AUClast of armodafinil in blood, demonstrating that the absorption of armodafinil was promoted by the aqueous solution of the compound and AIC hydrogel. Compared with AIC aqueous solution, AIC hydrogel had lower Cmax but higher AUClast and later Tmax, demonstrating that the AIC hydrogel dosage form was well absorbed and bioavailable in mice, which advantage may be related to the slow-release effect of the hydrogel.

The standard curves of armodafinil in blank homogenates of brain and liver were evaluated. The actual concentration obtained from different amounts of armodafinil input was used as the horizontal coordinate x, and the measured amount of armodafinil by LC-MS/MS was used as the vertical coordinate y. The linearity of armodafinil concentration in brain and liver tissue was investigated. The standard curve in mouse brain tissue homogenate was $y = 0.9285x + 69.801$ ($r = 0.999$); the standard curve in mouse liver tissue homogenate was $y = 0.9792x + 81.037$ ($r = 0.999$). Both standard curves had a good linear relationship.

From the *in-vivo* tissue distribution parameters (Table 5) and the drug-time curves (Fig. 15B), the Tmax of armodafinil ingredient in raw armodafinil, AIC aqueous solution and AIC hydrogel in mouse's brain were 0.50 h; the Cmax of armodafinil ingredient of three preparations in brain tissue was 258.78 ng/mL, 841.89 ng/mL and 1565.03 ng/mL, respectively; the AUClast was 1090.76 h ng/mL, 1501.47 h ng/mL and 4861.25 h ng/mL, respectively. From the parameters (Table 5) and the drug-time curves (Fig. 15C), the Tmax of armodafinil ingredient in raw armodafinil, AIC aqueous solution and AIC hydrogel in mouse's liver were 0.50 h, 0.17 h and 0.50 h, respectively; the Cmax of armodafinil ingredient of three preparations in liver tissue was 1151.18 ng/mL, 2966.91 ng/mL and 3590.17 ng/mL, and the AUClast was 2378.63 h ng/mL, 4568.03 h ng/mL and 11352.08 h ng/mL, respectively. The Cmax and AUClast of armodafinil of AIC hydrogel in brain and liver were larger, which proved that the AIC hydrogel had better effect of promoting the absorption of armodafinil.

The drug targeting index (DTI) of AIC hydrogel compared to armodafinil and AIC aqueous solution in terms of intracerebral delivery was calculated based on plasma pharmacokinetic and brain tissue distribution data in mice according to the following equation (Meng et al., 2018).

$$DTI1 = \frac{(AUC_{\text{brain}}/AUC_{\text{plasma}})_{\text{AIC hydrogel}}}{(AUC_{\text{brain}}/AUC_{\text{plasma}})_{\text{armodafinil}}}$$

$$DTI2 = \frac{(AUC_{\text{brain}}/AUC_{\text{plasma}})_{\text{AIC hydrogel}}}{(AUC_{\text{brain}}/AUC_{\text{plasma}})_{\text{AIC aqueous solution}}}$$

The DTI1 of AIC hydrogel nasal administration compared to raw armodafinil gavage was calculated to be 1.62, and the DTI2 of AIC hydrogel compared to AIC aqueous solution was calculated to be 2.39. The AIC hydrogel nasal administration not only allowed more armodafinil to enter the blood and tissues at the same dose, but also improved the tissue distribution structure in the body, allowing a higher proportion of armodafinil to enter the brain tissue, and provided a better choice for the treatment of PTSD in terms of dosage form and delivery method.

4. Conclusions

In this study, the HPLC of armodafinil was developed, and the optimal preparation method of AIC was explored by molecular dynamic simulation & docking and phase solubility measurement, and then was validated by IR and DSC. This experiment also evaluated the mucosal penetration of AIC aqueous solution, the release curve of AIC hydrogel in an *in-vitro* release determination, and the rheological data of AIC in an *in-vitro* simulated nasal environment. The safety of AIC hydrogel was also evaluated. The inescapable foot shock stimulation method was used for the preparation of the PTSD model, and the hypothesis that armodafinil may act as a stimulant, resulting in excellent behavioral parameters and a false-positive therapeutic effect was ruled out through two behavioral tests in mice during and after administration. The plasma CORT levels in AIC Hydrogel and AIC Aqueous Solution groups were normalized after drug withdrawal, and the expression of BDNF in the hippocampus was normalized. Immunohistochemical sections suggested that armodafinil could exert its therapeutic effect on PTSD by inhibiting DAT in the amygdala. Compared with Sertraline, armodafinil had not only a symptomatic relief but also a fundamental therapeutic effect on PTSD patients. AIC hydrogel had a better early therapeutic effect on PTSD than AIC aqueous solution because it had a better slow release, increased plasma CORT levels to a greater extent, inhibited DAT expression in the amygdala of mice, and achieved behavioral results that were not statistically different from those of the Healthy group in the freezing response test and open field test. The fluorescence imaging characteristics of Cy7 hydrogel after nasal administration showed that compared with the oral absorption method, nasal administration had the characteristics of forming high local concentration with the same dosage of drug and had better drug osmotic pressure potential. The pharmacokinetic characteristics and *in-vivo* distribution of different preparations of armodafinil showed that nasal administration of AIC hydrogel for the treatment of PTSD could not only allow more armodafinil to enter the blood and tissues and promote drug absorption, but also improve the tissue distribution structure of the drug *in-vivo*, allowing a higher proportion of Armodafinil to enter brain tissue for the purpose of brain targeting therapy. In summary, the AIC hydrogel provides a new option for the treatment of PTSD.

Declaration of Competing Interest

The authors declare that they have no known competing financial interests or personal relationships that could have appeared to influence the work reported in this paper.

Acknowledgement

This work was supported by the Beijing Natural Science Foundation [grant number 7202147].

References

- Bali, A., Jaggi, A.S., 2015. Electric foot shock stress: a useful tool in neuropsychiatric studies. *Rev. Neurosci.* 26 (6), 655–677.
- Bittencourt, V.C.E., Moreira, A., da Silva, J.G., Gomides, A.F.F., Velloso-Rodrigues, C., Kelmann, R.G., Mendonça, L.M., Lula, I.S., Denadai, A., M.L., 2019. Hydrophobic nanoprecipitates formed by benzoylphenylureas and β -cyclodextrin inclusion compounds: synthesis, characterization and toxicity against aedes aegypti larvae. *Helvion* 5(7), e02013.
- Chandasana, H., Kast, J., Bittman, J.A., Derendorf, H., 2018. Quantitative determination of armodafinil in human plasma by liquid chromatography-electrospray mass spectrometry: Application to a clinical study. *Biomed. Chromatogr.* 32 (11), e4342.
- Chapman, J.L., Vakulin, A., Hedner, J., Yee, B.J., Marshall, N.S., 2016. Modafinil/armodafinil in obstructive sleep apnoea: a systematic review and meta-analysis. *Eur. Respir. J.* 47 (5), 1420–1428.
- Chu, K., Chen, L., Xu, W., Li, H., Zhang, Y., Xie, W., Zheng, J., 2013. Preparation of a paeonol-containing temperature-sensitive in situ gel and its preliminary efficacy on allergic rhinitis. *Int. J. Mol. Sci.* 14 (3), 6499–6515.
- Cooper, A.A., Zoellner, L.A., Roy-Byrne, P., Mavissakalian, M.R., Feeny, N.C., 2017. Do changes in trauma-related beliefs predict PTSD symptom improvement in prolonged exposure and sertraline? *J. Consult. Clin. Psychol.* 85 (9), 873–882.
- Darwish, M., Kirby, M., Hellriegel, E.T., 2009. Comparison of steady-state plasma concentrations of armodafinil and modafinil late in the day following morning administration: post hoc analysis of two randomized, double-blind, placebo-controlled, multiple-dose studies in healthy male subjects. *Clin. Drug. Investig.* 29 (9), 601–612.
- Davis, M.E., Brewster, M.E., 2004. Cyclodextrin-based pharmaceuticals: past, present and future. *Nat. Rev. Drug Discov.* 3 (12), 1023–1035.
- Destruel, P.L., Zeng, N., Seguin, J., Douat, S., Rosa, F., Brignole-Baudouin, F., Dufay, S., Dufay-Wojcicki, A., Maury, M., Mignet, N., Boudy, V., 2020. Novel in situ gelling ophthalmic drug delivery system based on gellan gum and hydroxyethylcellulose: Innovative rheological characterization, in vitro and in vivo evidence of a sustained precorneal retention time. *Int. J. Pharm.* 574, 118734.
- Dimatteo, R., Darling, N.J., Segura, T., 2018. In situ forming injectable hydrogels for drug delivery and wound repair. *Adv. Drug Deliv. Rev.* 127, 167–184.
- Du, Q., Du, S.Y., Li, P.Y., Lu, Y., Bai, J., Teng, H.H., Wang, Z., Zhang, Q., 2016. Effect of salivianolic acid B on nasal absorption in rats in situ. *Zhongguo Zhong Yao Za Zhi* 41 (2), 303–308.
- Feduccia, A.A., Jerome, L., Yazar-Klosinski, B., Emerson, A., Mithoefer, M.C., Doblin, R., 2019. Breakthrough for trauma treatment: safety and efficacy of MDMA-assisted psychotherapy compared to paroxetine and sertraline. *Front Psychiatry.* 10, 650.
- Ferland, C.L., Reichel, C.M., McGinty, J.F., 2016. Effects of oxytocin on methamphetamine-seeking exacerbated by predator odor pre-exposure in rats. *Psychopharmacology (Berl.)* 233 (6), 1015–1024.
- Ghose, A.K., Herberich, T., Hudkins, R.L., Dorsey, B.D., Mallamo, J.P., 2012. Knowledge-Based, Central Nervous System (CNS) lead selection and lead optimization for CNS drug discovery. *ACS Chem. Neurosci.* 3 (1), 50–68.
- Gizurarson, S., 2015. The effect of cilia and the mucociliary clearance on successful drug delivery. *Biol. Pharm. Bull.* 38 (4), 497–506.
- Hamidovic, A., Khafaja, M., Brandon, V., Anderson, J., Ray, G., Allan, A.M., Burge, M.R., 2017. Reduction of smoking urges with intranasal insulin: a randomized, crossover, placebo-controlled clinical trial. *Mol. Psychiat.* 22 (10), 1413–1421.
- Kumaki, Y., Salazar, A.M., Wandersee, M.K., Barnard, D.L., 2017. Prophylactic and therapeutic intranasal administration with an immunomodulator, Hiltonol[®] (Poly IC:LC), in a lethal SARS-CoV-infected BALB/c mouse model. *Antiviral Res.* 139, 1–12.
- Kuniishi, H., Ichisaka, S., Yamamoto, M., Ikubo, N., Matsuda, S., Futora, E., Harada, R., Ishihara, K., Hata, Y., 2017. Early deprivation increases high-leaning behavior, a novel anxiety-like behavior, in the open field test in rats. *Neurosci. Res.* 123, 27–35.
- Li, W., Ma, Y.-B., Yang, Q.-i., Li, B.-L., Meng, Q.-G., Zhang, Y.-i., 2017. Effect and safety of sertraline for treat posttraumatic stress disorder: a multicenter randomised controlled study. *Int. J. Psychiat. Clin. Pract.* 21 (2), 151–155.
- Lochhead, J.J., Thorne, R.G., 2012. Intranasal delivery of biologics to the central nervous system. *Adv. Drug Deliv. Rev.* 64 (7), 614–628.
- Louvar, H., Maccari, S., Ducrocq, F., Thomas, P., Darnaudéry, M., 2005. Long-term behavioural alterations in female rats after a single intense footshock followed by situational reminders. *Psychoneuroendocrinology* 30 (4), 316–324.
- Meng, Q., Wang, A., Hua, H., Jiang, Y., Wang, Y., Mu, H., Wu, Z., Sun, K., 2018. Intranasal delivery of Huperzine A to the brain using lactoferrin-conjugated N-trimethylated chitosan surface-modified PLGA nanoparticles for treatment of Alzheimer's disease. *Int. J. Nanomed.* 13, 705–718.
- Nair, A.B., Jacob, S., 2016. A simple practice guide for dose conversion between animals and human. *J. Basic Clin. Pharm.* 7 (2), 27–31.
- Niemczyk-Soczynska, B., Grady, A., Kolbuk, D., Krzton-Maziopa, A., Sajakiewicz, P., 2019. Crosslinking kinetics of methylcellulose aqueous solution and its potential as a scaffold for tissue engineering. *Polymers (Basel)* 11 (11), 1772. <https://doi.org/10.3390/polym11111772>.
- Nishimura, T., Kaneko, A., 2019. Temperature profile of the nasal cavity in Japanese macaques. *Primates* 60 (5), 431–435.
- Pang, L., Zhu, S., Ma, J., Zhu, L., Liu, Y., Ou, G.-e., Li, R., Wang, Y., Liang, Y.-i., Jin, X.-u., Du, L., Jin, Y., 2021. Intranasal temperature-sensitive hydrogels of cannabidiol inclusion complex for the treatment of post-traumatic stress disorder. *Acta Pharm. Sin.* B 11 (7), 2031–2047.
- Pawlyk, A.C., Jha, S.K., Brennan, F.X., Morrison, A.R., Ross, R.J., 2005. A rodent model of sleep disturbances in posttraumatic stress disorder: the role of context after fear conditioning. *Biol. Psychiat.* 57 (3), 268–277.
- Pynoos, R.S., Ritzmann, R.F., Steinberg, A.M., Goenjian, A., Prisecaru, I., 1996. A behavioral animal model of posttraumatic stress disorder featuring repeated exposure to situational reminders. *Biol. Psychiat.* 39 (2), 129–134.
- Rauch, S.A.M., Kim, H.M., Powell, C., Tuerk, P.W., Simon, N.M., Acierio, R., Allard, C. B., Norman, S.B., Venners, M.R., Rothbaum, B.O., Stein, M.B., Porter, K., Martis, B., King, A.P., Liberzon, I., Phan, K.L., Hoge, C.W., 2019. Efficacy of prolonged exposure therapy, sertraline hydrochloride, and their combination among combat veterans with posttraumatic stress disorder: a randomized clinical trial. *JAMA Psychiat.* 76 (2), 117–126.
- Sahin-Yilmaz, A., Naclerio, R.M., 2011. Anatomy and physiology of the upper airway. *Proc. Am. Thorac. Soc.* 8 (1), 31–39.
- Sartori, S.B., Singewald, N., 2019. Novel pharmacological targets in drug development for the treatment of anxiety and anxiety-related disorders. *Pharmacol. Ther.* 204, 107402.
- Schöner, J., Heinz, A., Endres, M., Gertz, K., Kronenberg, G., 2017. Post-traumatic stress disorder and beyond: an overview of rodent stress models. *J. Cell Mol. Med.* 21 (10), 2248–2256.
- Stübner, S., Grohmann, R., Greil, W., Zhang, X., Müller-Oerlinghausen, B., Bleich, S., Rüter, E., Möller, H.J., Engel, R., Falkai, P., Toto, S., Kasper, S., Neyazi, A., 2018. Suicidal ideation and suicidal behavior as rare adverse events of antidepressant medication: current report from the AMSP multicenter drug safety surveillance project. *Int. J. Neuropsychopharmacol.* 21 (9), 814–821.
- Swain, G.P., Patel, S., Gandhi, J., Shah, P., 2019. Development of Moxifloxacin Hydrochloride loaded in-situ gel for the treatment of periodontitis: In-vitro drug release study and antibacterial activity. *J. Oral. Biol. Craniofac. Res.* 9 (3), 190–200.
- Takalkar, D., Desai, N., 2018. Nanolipid gel of an antimycotic drug for treating vulvovaginal candidiasis-development and evaluation. *AAPS PharmSciTech.* 19 (3), 1297–1307.
- Tanaka, M., Li, H., Zhang, X., Singh, J., Dalgard, C.L., Wilkerson, M., Zhang, Y., 2019. Region- and time-dependent gene regulation in the amygdala and anterior cingulate cortex of a PTSD-like mouse model. *Mol. Brain* 12 (1), 25.
- Thorne, R.G., Hanson, L.R., Ross, T.M., Tung, D., Frey 2nd, W.H., 2008. Delivery of interferon-beta to the monkey nervous system following intranasal administration. *Neuroscience* 152 (3), 785–797.
- Xiao, H., Li, H., Song, H., Kong, L., Yan, X., Li, Y., Deng, Y., Tai, H., Wu, Y., Ni, Y., Li, W., Chen, J., Yang, J., 2020. Shenao jiannao oral liquid, an herbal formula, ameliorates cognitive impairments by rescuing neuronal death and triggering endogenous neurogenesis in AD-like mice induced by a combination of A β 42 and scopolamine. *J. Ethnopharmacol.* 259, 112957.
- Zoladz, P.R., Fleshner, M., Diamond, D.M., 2012. Psychosocial animal model of PTSD produces a long-lasting traumatic memory, an increase in general anxiety and PTSD-like glucocorticoid abnormalities. *Psychoneuroendocrinology* 37 (9), 1531–1545.